#50 11/18/80

MASTER

Ho. 582

DOE/JPL/954817-4

EPITAXIAL SILICON GROWTH FOR SOLAR CELLS

Final Report

By
R. V. D'Aiello
P. H. Robinson
D. Richman

April 1979

Work Performed Under Contract No. NAS-7-100-954817

RCA Laboratories
Princeton, New Jersey

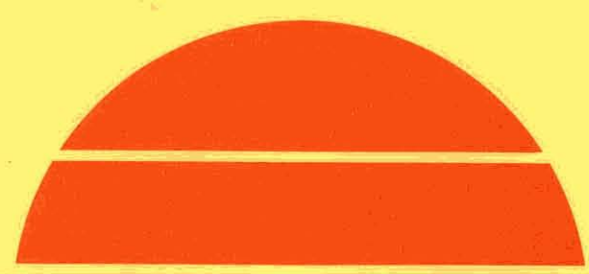

U.S. Department of Energy

DISTRIBUTION OF THIS DOCUMENT IS UNLIMITED

Solar Energy

DISCLAIMER

This report was prepared as an account of work sponsored by an agency of the United States Government. Neither the United States Government nor any agency Thereof, nor any of their employees, makes any warranty, express or implied, or assumes any legal liability or responsibility for the accuracy, completeness, or usefulness of any information, apparatus, product, or process disclosed, or represents that its use would not infringe privately owned rights. Reference herein to any specific commercial product, process, or service by trade name, trademark, manufacturer, or otherwise does not necessarily constitute or imply its endorsement, recommendation, or favoring by the United States Government or any agency thereof. The views and opinions of authors expressed herein do not necessarily state or reflect those of the United States Government or any agency thereof.

DISCLAIMER

Portions of this document may be illegible in electronic image products. Images are produced from the best available original document.

NOTICE

This report was prepared as an account of work sponsored by the United States Government. Neither the United States nor the United States Department of Energy, nor any of their employees, nor any of their contractors, subcontractors, or their employees, makes any warranty, express or implied, or assumes any legal liability or responsibility for the accuracy, completeness or usefulness of any information, apparatus, product or process disclosed, or represents that its use would not infringe privately owned rights.

This report has been reproduced directly from the best available copy.

Available from the National Technical Information Service, U. S. Department of Commerce, Springfield, Virginia 22161.

Price: Paper Copy $5.25
Microfiche $3.00

DOE/JPL/954817-4
Distribution Category UC-63b

DRL Line Item No. 10

DISCLAIMER
This book was prepared as an account of work sponsored by an agency of the United States Government. Neither the United States Government nor any agency thereof, nor any of their employees, makes any warranty, express or implied, or assumes any legal liability or responsibility for the accuracy, completeness, or usefulness of any information, apparatus, product, or process disclosed, or represents that its use would not infringe privately owned rights. Reference herein to any specific commercial product, process, or service by trade name, trademark, manufacturer, or otherwise, does not necessarily constitute or imply its endorsement, recommendation, or favoring by the United States Government or any agency thereof. The views and opinions of authors expressed herein do not necessarily state or reflect those of the United States Government or any agency thereof.

EPITAXIAL SILICON GROWTH FOR SOLAR CELLS

R. V. D'Aiello, P. H. Robinson,
and D. Richman

RCA Laboratories
Princeton, New Jersey 08540

FINAL REPORT

April 1979

This work was performed for the Jet Propulsion Laboratory, California Institute of Technology, under NASA Contract NAS7-100 for the U. S. Department of Energy.

JPL Low-cost Silicon Solar Array Project is funded by DOE and forms part of the Photovoltaic Conversion Program to initiate a major effort toward the development of low-cost solar arrays.

Prepared Under Contract No. 954817
JET PROPULSION LABORATORY
CALIFORNIA INSTITUTE OF TECHNOLOGY
Pasadena, California 91103

DISTRIBUTION OF THIS DOCUMENT IS UNLIMITED

PREFACE

This Final Report, prepared by RCA Laboratories, Princeton, NJ 08540, describes work performed for the period 1 October 1977 through 31 September 1978, under Contract No. 954817 in the Energy Systems Research Laboratory, B. F Williams, Director. D. Richman is the Group Head and the Project Supervisor. R. V. D'Aiello is the Project Scientist. Others who participated in the research and/or writing of this report are Y. S. Chiang (epitaxial growth) and B. W. Faughnan (diagnostic measurements). The RCA Report No. is PRRL-79-CR-13.

The JPL Project Monitor is A. Kachere.

TABLE OF CONTENTS

Section | Page

I. SUMMARY 1

II. INTRODUCTION 3

III. BASELINE EPITAXIAL SOLAR CELLS ON SINGLE-CRYSTAL SILICON SUBSTRATES 5

A. Epitaxial Growth Procedures 5

1. Epitaxial Reactor 5
2. Epitaxial Growth 5

B. Solar-Cell Fabrication 6

1. General Procedures 6
2. Mask Design 7
3. Metallization 8
4. Antireflection Coating 8
5. Mesa Etching 8

C. Solar-Cell Measurements 9

1. I-V Measurements 9
2. Quantum Efficiency Measurements 11

D. Baseline Epitaxial Solar-Cell Structures 11

IV. EPITAXIAL SOLAR CELLS ON LOW-COST SILICON SUBSTRATES 15

A. Epitaxial Growth and Solar Cells on Polycrystalline Silicon 15

1. Material Characterization 15
2. Epitaxial Solar Cells - Diffused Junctions 18
3. Epitaxial Solar Cells - Grown Junctions 20

B. Epitaxial Solar Cells on Union Carbide RMS Silicon 20

1. Material Characterization 20
2. Solar-Cell Results - Diffused-Epitaxial Structures 21
3. All-Epitaxial Cells on RMS Substrates 21

C. Dow Corning Upgraded Metallurgical Grade Silicon 28

1. Material Characterization 28
2. Diffused-Epitaxial Solar Cells 32
3. All-Epitaxial Solar Cells 36

TABLE OF CONTENTS (Continued)

Section

D. Crystal Systems Cast Silicon Substrates 36

1. Material Characterization 36

2. Solar-Cell Results 38

E. Discussion of Results 39

F. Summary 41

V. ADVANCED EPITAXIAL REACTORS 42

VI. COST ANALYSIS 48

VII. CONCLUSIONS AND RECOMMENDATIONS 52

REFERENCES 54

APPENDIX - SOLAR CELLS ON TITANIUM-DOPED SUBSTRATES 55

LIST OF ILLUSTRATIONS

Figure		Page
1.	Milestone plan for overall program	4
2.	Solar-cell mask design including diagnostic cells	7
3.	Reflection and absorption properties of spin-on titaniumsilica film as a function of wavelength	9
4.	I-V measuring apparatus	10
5.	Quantum efficiency measuring apparatus	12
6.	Concentration profile of epitaxial base layer	13
7.	Comparison of the surfaces of 35-μm epitaxial layers grown on (a) polished and (b) etched Wacker polycrystalline substrate	16
8.	150-μm-thick film grown on chemically etched substrate. (a) Transmission and (b) section topographs	17
9.	Enlarged portion of the section topograph (Fig. 8)	18
10.	Projection x-ray topographs of two sections of Union Carbide RMS silicon	22
11.	A series of section topographs of Union Carbide RMS silicon, taken at 1-mm spacings in the large grain at lower right of Fig. 10. Layer is at left edge of each topograph	23
12.	Enlargement of several sections of topographs in Fig. 11. Layer is at upper left of each topograph	24
13.	Illuminated I-V curve for sample X-13 RMS	26
14.	Spectral response curves for diffused-epitaxial structure on Union Carbide RMS silicon, sample X-13	27
15.	Spectral response curves for diffused epitaxial structure on Union Carbide RMS silicon, sample X-14	28
16.	Spectral response curves for diffused epitaxial structure on Union Carbide RMS silicon, sample X-15	29
17.	Spectral response curves for all-epitaxial cells on Union Carbide RMS silicon	30
18.	Projection x-ray topograph of a 100-μm-thick epitaxial layer grown on Dow Corning upgraded metallurgical grade silicon	31
19.	Section x-ray topographs of the crystal in Fig. 18 showing the epitaxial layer (at the right) and the substrate. The dark strain bands in between result from misfit dislocations	33

LIST OF ILLUSTRATIONS (Continued)

Figure — Page

20. Junction I-V characteristics and parameters for diffused-epitaxial solar cells on Union Carbide RMS silicon (X-14) and on Dow Corning silicon (25-3) 34
21. Spectral response curves for three diffused-epitaxial solar cells and a bulk cell fabricated on Dow Corning silicon ... 35
22. Spectral response curves for all-epitaxial solar cells on Dow Corning silicon 37
23. Section topograph, Crystal Systems silicon 38
24. Rotary Disc reactor and conventional epitaxial reactor 43
25. Assembled version of prototype Rotary Disc reactor 44

LIST OF TABLES

Table — Page

1. AM-1 Characteristics of Baseline Diffused-Epitaxial Structures on Single-Crystal Substrates 13
2. AM-1 Characteristics of Baseline All-Epitaxial Solar-Cell Structures 14
3. Characteristics of Low-Cost Silicon Substrates 15
4. Summary of Solar-Cell Data for Epitaxial Structures 19
5. Summary of Cell Performance for All-Epitaxially Grown Structures on Polycrystalline Wacker Substrates 20
6. Measured Solar-Cell and Structural Parameters for Diffused-Epitaxial Structures on Union Carbide RMS Silicon 25
7. Summary of All-Epitaxial Structures n/p/p Grade/p^+ on Union Carbide RMS Silicon Substrate 29
8. Summary of AM-1 Cell Parameters for Diffused-Epitaxial Solar Cells on Dow Corning Upgraded Metallurgical Silicon Substrates ... 34
9. AM-1 Solar-Cell Parameters for All-Epitaxial Structures on Dow Corning Upgraded Metallurgical Silicon Substrates 36
10. Summary of AM-1 Solar-Cell Parameters for Cells on Crystal Systems Silicon 40
11. Summary of the Characteristics of All-Epitaxial Solar Cells Grown in the Rotary Disc Reactor on Dow Substrates 46
12. Process Parameters: Epitaxy 49
13. Cost Analysis: Epitaxial Solar Panel 50

SECTION I

SUMMARY

The objectives of this contract were

- To determine the feasibility of silicon epitaxial growth on low-cost silicon substrates for the development of silicon sheet capable of producing low-cost, high-efficiency solar cells.
- To achieve a goal of 12% (AM-0) efficient solar cells fabricated on thin epitaxial layers (<25 μm) grown on low-cost substrates.
- To evaluate the add-on cost for the epitaxial process and to develop low-cost epitaxial growth procedures for application in conjunction with low-cost silicon substrates.

In Section III, the basic epitaxial procedures and solar-cell fabrication and evaluation techniques are described, followed by a discussion of the development of baseline epitaxial solar-cell structures, grown on high-quality conventional silicon substrates. This work resulted in the definition of three basic structures which reproducibly yielded efficiencies in the range of 12 to 13.7%.

These epitaxial growth procedures and baseline structures were then used to grow diagnostic layers and solar cells on four potentially low-cost silicon substrates. A description of the crystallographic properties of such layers and the performance of epitaxially grown solar cells fabricated on these materials is given in Section IV. The major results were the achievement of cell efficiencies of 10.6 to 11.2% on multigrained substrates and $\sim$13% on a low-cost single-crystal substrate.

In Section V, an advanced epitaxial reactor, the Rotary Disc, is described. The results of growing solar-cell structures of the baseline type and on low-cost substrates are given.

The add-on cost for the epitaxial process is assessed in Section VI. These cost estimates show a value of $\sim$0.46/W using existing or near-term technologies and project an add-on cost of $0.10/W for future reactors. The economic advantages of the epitaxial process as they relate to silicon substrate selection are also discussed.

The major conclusions drawn from this work and recommendations for the further development needed to achieve the ultimate cost goals are given in Section VII.

An appendix is included describing the effect of titanium in substrates on epitaxial and bulk-cell performance.

SECTION II

INTRODUCTION

The high cost of the starting silicon hampers the establishment of the elements of a manufacturing process for large-scale production of solar panels at a projected cost of under $0.50/W. Accordingly, lower cost techniques for the reduction and purification of silicon are under development by several silicon manufacturers [1,2]. However, these processes often result in polycrystalline forms of silicon containing unwanted impurities and defects. Efficiencies of solar cells made directly into this material have been low, and some of the still lower cost forms of simply purified metallurgical grade silicon are not suitable for the direct fabrication of solar cells. Regardless of how low the cost of the starting silicon is, it is important in most applications from a system-cost viewpoint to obtain as high a cell efficiency as possible, with the 12 to 15% range being a desirable target.

The approach to this problem taken in this contract work is the use of thin epitaxial films grown on low-cost silicon. This approach has a number of already demonstrated technical advantages and utilizes a technology in which RCA has a great deal of experience [3,4]. The advantages of epitaxy are substantial, even exclusive of cost, since it is a method whereby dopant distributions and the structure of the grown silicon layer and its thickness can be readily adjusted to obtain a desired objective. However, epitaxy as it is practiced in the semiconductor industry today is an expensive process because of high labor involvement, batch processing, and the inefficient use of electricity and chemicals. This program was directed toward demonstrating the technical feasibility of epitaxial growth on low-cost silicon substrates for

---

1. L. P. Hunt, V. D. Dosaj, and J. R. McCormick, "Advances in the Dow-Corning Process for Silicon," Proc. 13th IEEE Photovoltaic Specialists Conference, June 1978.
2. W. C. Breneman, F. G. Farrier, and H. Morihara, "Preliminary Process Design and Economics of Low-Cost Solar-Grade Silicon Production," Proc. 13th IEEE Photovoltaic Specialists Confernece, June 1978.
3. R. V. D'Aiello, P. H. Robinson, and H. Kressel, "Epitaxial Silicon Solar Cells," Appl. Phys. Lett. 28, 231 (1976).
4. H. Kressel, R. V. D'Aiello, E. R. Levin, P. H. Robinson, and S. H. McFarlane, "Epitaxial Silicon Solar Cells on Ribbon Substrates," J. Cryst. Growth 39, 23 (1977).

application in producing low-cost, efficient solar cells. The economic constraints also required continual cost analysis and development of low-cost epitaxial procedures and reactor systems.

The program milestone plan which guided this work is shown in Fig. 1.

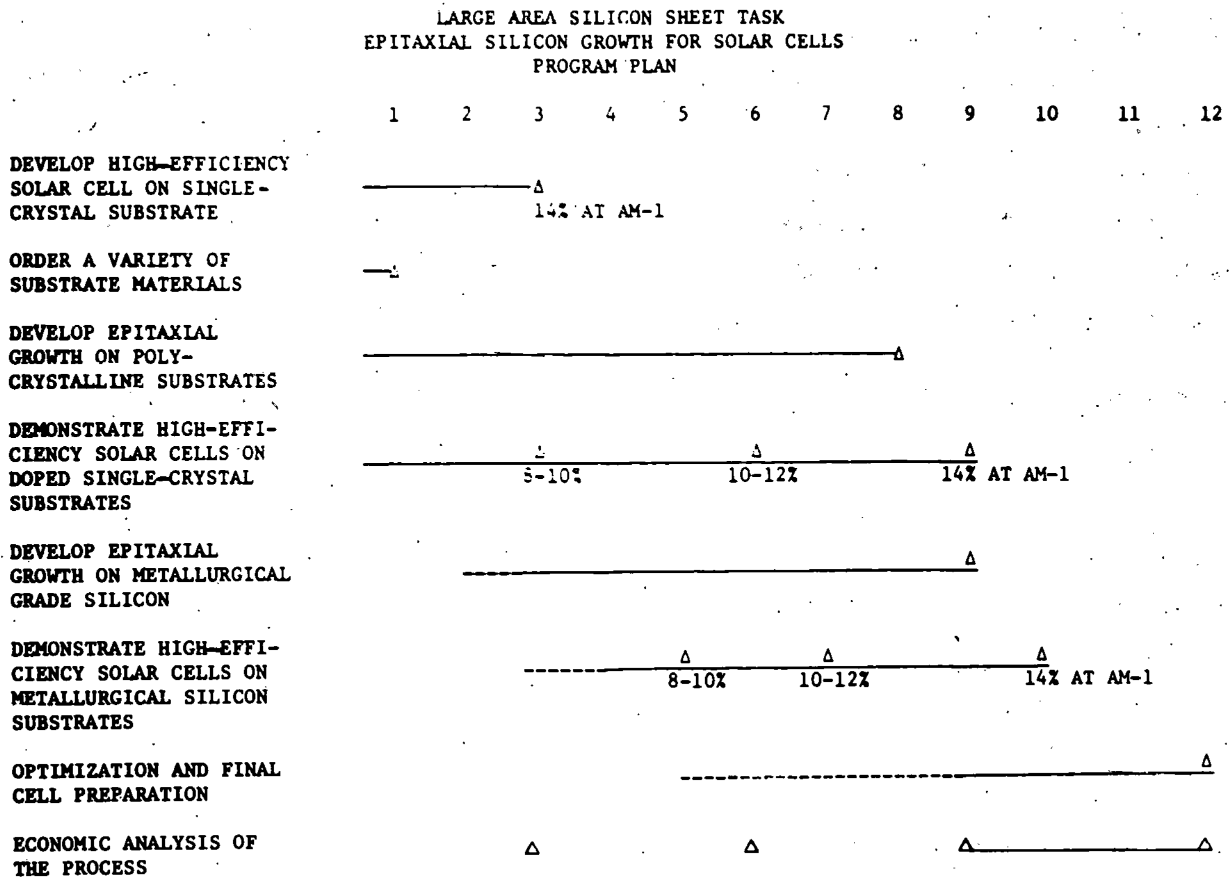

Figure 1. Milestone plan for overall program

SECTION III

BASELINE EPITAXIAL SOLAR CELLS ON SINGLE-CRYSTAL SILICON SUBSTRATES

A. EPITAXIAL GROWTH PROCEDURES

The epitaxial reactor and growth procedures described here were used to establish baseline solar-cell structures and material properties of the grown layers on both single-crystal and several potential low-cost silicon substrates. These procedures apply to the results described in Sections III and IV; in Section V a description is given and data are presented for structures grown in a prototype model of an advanced reactor design, the Rotary Disc (RD) reactor, which encompasses the features required to make the epitaxial method economically feasible.

1. Epitaxial Reactor

The growths were carried out using dichlorosilane in a standard horizontal reactor. The quartz tube has a cross section of 5 x 10 cm and held a silicon carbide-coated graphite susceptor that was 30 cm long. Heating was accomplished by rf induction into the susceptor, which was inclined horizontally, and the walls of the reactor were air-cooled. Hydrogen was obtained from a Pd-Ag diffusion cell. Doping gases were arsine or diborane diluted with hydrogen at the 10- to 20-ppm level and were further diluted as needed before they were inserted into the reactant gas stream. Dichlorosilane was metered as a gas directly from the cylinder and temperatures were measured with an optical pyrometer and corrected for emissivity and quartz adsorption effects.

2. Epitaxial Growth

The silicon substrates used for epitaxial growth are:

(1) Cleaned for 10 min in boiling ammonia-peroxide-water mixtures (reagent ratio 4-1-1).

(2) Rinsed in super q water (filtered de-ionized water with a resistivity greater than 15 MΩ).

(3) Cleaned for 10 min in boiling hydrogen chloride-peroxide-water mixtures (reagent ratio 4-1-1).

(4) Rinsed in super q water.

(5) Substrates are then spun dry and placed on a susceptor which is inserted into epitaxial reactor.

(6) Reactor is flushed with hydrogen, flow rate 30 liter/min, for 10 min. All other lines to be used are flushed to vent line for 5 min and turned off.

(7) Rf generator is turned on and substrates heated to 1150°C with hydrogen flowing for 5 min.

(8) Substrates are etched in 1% HCl for 5 min at 1150°C; this removes about 5 μm of material.

(9) HCl turned off and system flushed with hydrogen for 5 min.

(10) Temperature of substrates reduced to growth temperature 1100°C.

(11) Flow rates of gases (SiH_2Cl_2, AsH_3, or B_2H_6) to give desired growth rate and doping level and conductivity type are metered to vent line.

(12) Automatic timer set to give predetermined thickness, and growth is started.

(13) Growth stopped automatically and reactor flushed with hydrogen for 3 min.

(14) Rf power turned off and system cooled with hydrogen flowing.

B. SOLAR-CELL FABRICATION

In this section, the details of the solar-cell fabrication starting from as-grown epitaxial wafers are described.

1. General Procedures

The general procedures for fabrication of the solar cells and test structures are:

(1) Grow epitaxial layers - 3 wafers/run.

(2) Characterize spreading resistance.

(3) Clean wafers - $H_2SO_4:H_2O_2$; $H_2O_2:NH_3OH$; H_2O_2:HCl boiling solutions.

For epitaxial structures without a junction layer: $POCl_3$ diffusion at 875°C for 30 min followed by a slow pull (10 min). Wafers are then stripped of oxide and a four-point sheet resistance measurement is made.

(4) Metallize by evaporation of Ti/Ag (0.2 μm/5 μm) - front and back.

(5) Spin-on AR coating - bake and sinter.

(6) Screen-on wax to define cell and test structure areas.

(7) Etch silicon to form mesa structures delineating cell area.

(8) Remove wax, rinse, and bake.

These processing steps are described in more detail below.

2. Mask Design

The contact mask used to delineate the metallization pattern for all cells reported here is shown in Fig. 2. The large cell is 2 x 2 cm, having 11 current collecting fingers and a single bus-bar with a total 7% metal area coverage. The two small cells and ten diodes are for diagnostic purposes such as the measurement of lifetime and area dependence of electrical characteristics. The parallel bar structures A and A' are included for measurement of surface-layer sheet resistance and metal-to-silicon contact resistivity, and the line structure B is for the measurement of metal sheet resistance.

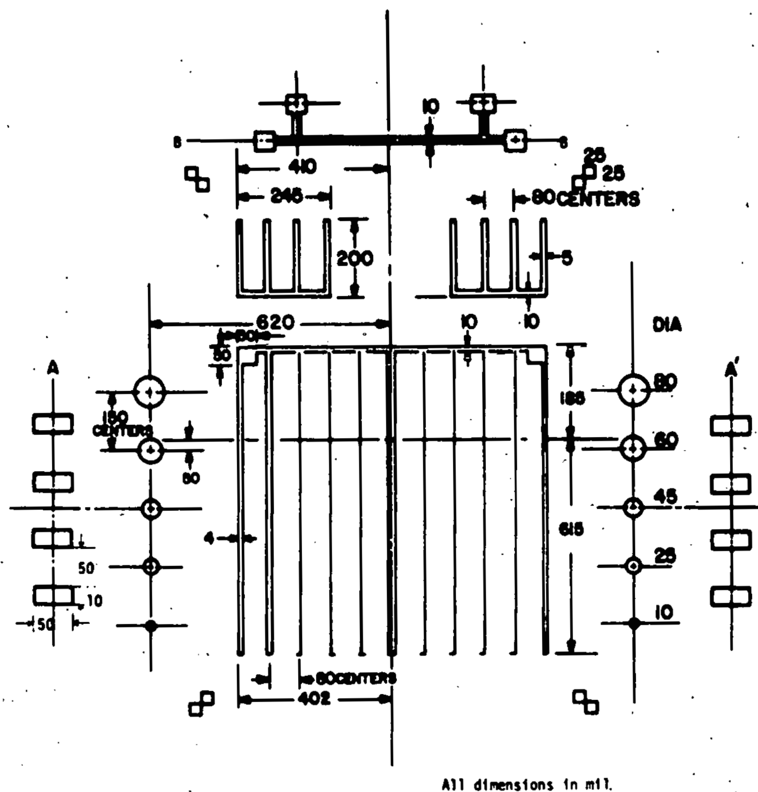

Figure 2. Solar-cell mask design including diagnostic cells.

3. Metallization

Metallization was done by E-gun evaporation of 0.2 μm of titanium followed by 5 μm of silver. These metals are evaporated over the entire front and back of the wafers and the pattern shown in Fig. 2 is then defined photolithographically. The silicon substrates were not heated during evaporation; sintering was done in a separate furnace at 500°C for 15 min in argon after the photoresist and metal etching.

4. Antireflection Coating

A commercially available* titaniumsilica film spin-on antireflection (AR) coating was used because of its ease in handling and good optical properties. The type-C spin-on film we purchased and used has a reported index of refraction of 1.96. The liquid is spun onto the silicon wafer and then baked successively at 100°C and 400°C for 15 min in air. The resulting thickness of the film depends upon the spin-speed, but saturates at ~765 Å for spin speeds greater than 6000 rpm.

In order to obtain thinner films with lower spin speeds, the liquid was diluted 75% liquid to 25% ethyl alcohol. With this solution, a spin speed of 4100 rpm yields a reproducible film thickness of 750 Å. The optical reflection and transmission properties were measured over the visible wavelength range. The measured reflection of a typical spin-on AR coating on a polished silicon surface is shown in the upper trace of Fig. 3. By making transmission measurements of similar films on quartz plates, absorption was estimated at less than 1% for wavelengths greater than 4000 Å and only 5% at 3500 Å. The measured absorption is shown in the lower trace in Fig. 3.

5. Mesa Etching

We use mesa etching to define the cell and test structure areas and to delineate and clean the peripheral junction areas. This is accomplished by screening a presoftened wax onto the wafers through a metal mask. The exposed silicon is then etched to a depth of 1 mil (25 μm) using a hydrofluoric acid, acetic acid, nitric acid (1:2:2) solution. The resulting cell area varies somewhat from run to run but is generally close to 4.4 cm^2. This process results in a clean, damage-free peripheral mesa area including the junction at the cell edge.

*Titaniumsilica film-type C, purchased from Emulsitone Co., Whippany, NJ.

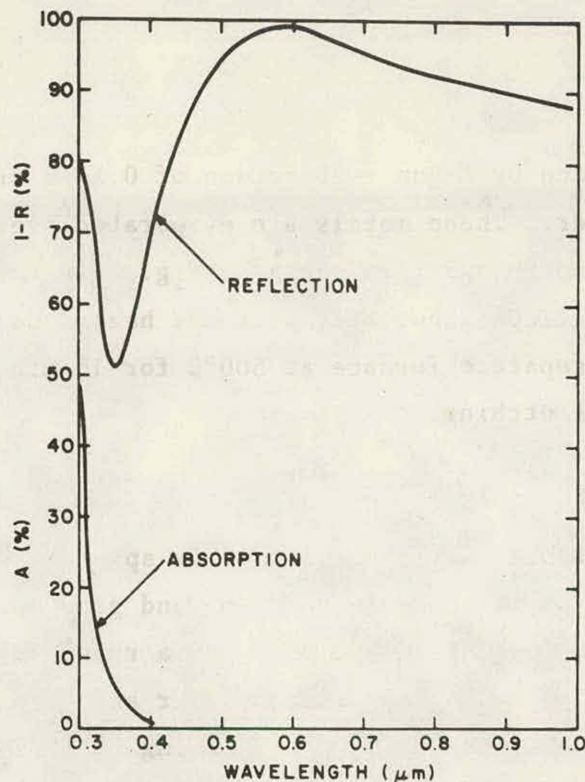

Figure 3. Reflection and absorption properties of spin-on titaniumsilica film as a function of wavelength.

C. SOLAR-CELL MEASUREMENTS

1. I-V Measurements

Figure 4 shows the apparatus used to measure I-V characteristics. Three 300-W ELH quartz-iodine lamps mounted on a photographic stand provide an approximately 3-in.-diameter circle of uniform light. The solar cell under test is mounted on a gold-plated copper baseplate by means of a vacuum hold-down. The metal baseplate forms one contact to the solar cell and is the system ground. The current and voltage contacts are made to the front side bus bar of the solar cell by means of flexible gold-ball-tipped metal fingers. The voltage contact is connected to the middle of the bus bar on the solar cell while two current contacts are used, one on either end of the bus bar.

The temperature of the cell is monitored by a thermocouple mounted underneath the solar cell in a groove in the baseplate. The temperature is kept at 28°C by a thermoelectric cooler attached to the baseplate. The lamps are powered from the ac lines through an auto-transformer. The voltage applied to the lamps is kept at 90 V to prolong the life of the ELH lamps (average life ~40 to 50 hours). The I-V and power-voltage curves are obtained from an

Figure 4. I-V measuring apparatus.

electronic circuit which sweeps a resistive load from zero to infinity across the solar cell in a few seconds. All the necessary calibration is provided in this box. Calibration of the lamps is obtained by placing a secondary standard solar cell, obtained from NASA-Lewis*, in the sample holder and setting the lamp-sample distance to give the short-circuit current appropriate for AM-1 conditions (100 mW/cm^2). Another standard cell is separately mounted on the sample baseplate and its short-circuit current is continuously monitored. Thus, if the lamp output changes slightly during a series of measurements, corrections can be made without remounting the standard cell.

2. Quantum Efficiency Measurements

The apparatus for measuring the quantum efficiency of solar cells is shown schematically in Fig. 5. The light from a tungsten lamp is passed through a chopper and brought to a focus on a narrow slit. The light emerging from the slit passes through one of 12 filters mounted on a rotatable filter wheel. The light is then collimated, passes through a beam splitter, and is then focused to a narrow image (1 x 8 mm) which fits between the metal fingers of the solar cell. A signal proportional to the current output from the cell is mounted on the output of the PAR** phase sensitive detector. At the same time, the other light beam from the beam splitter is detected by a Si photodetector which has been calibrated at each filter wavelength by comparison with the output from an NBS Standard Lamp. The whole system is calibrated by measuring the response of the Si photodetector at each of the filter wavelengths in both the sample and detector positions. In this way the absolute quantum efficiency of a solar cell can be obtained.

D. BASELINE EPITAXIAL SOLAR-CELL STRUCTURES

Since most low-cost silicon substrate forms developed to date are p-type (aluminum or boron residual impurity), a first step in our program plan involved the development of $n/p/p^+$ epitaxial structures. The work performed during the first two months of this contract was directed toward establishing the efficiency level and performance characteristics of $n^+/p/p^+$ epitaxial solar cells

*Standard (AM-1) silicon solar cells were supplied by H. W. Brandhorst, Jr. and C. Swartz of NASA-Lewis Research Center, Cleveland, OH.
**Princeton Applied Research Corp., Princeton, NJ.

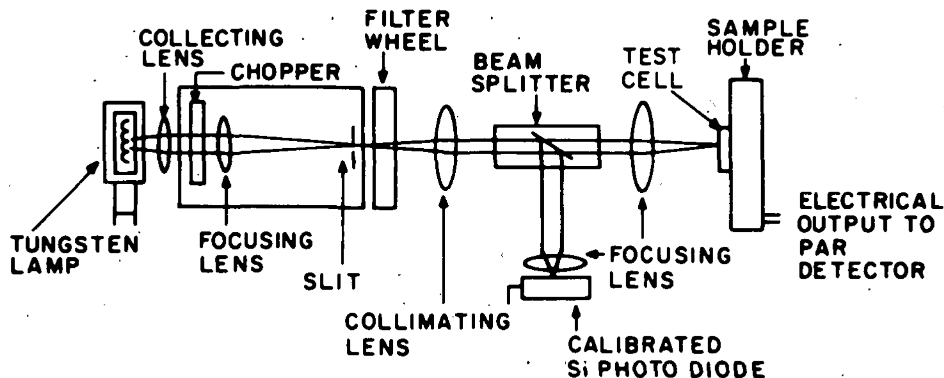

Figure 5. Quantum efficiency measuring apparatus.

grown on high-quality (conventional) single-crystal p^+ substrates. For reasons of economy in the epitaxial growth, thin structures in the 15- to 50-μm range were studied. The best of these structures then formed a baseline for later comparison to cells grown on low-cost silicon.

Initial studies were performed on $n^+/p/p\text{-graded}/p^+$ structures with the n^+ layer formed by diffusion. The growth of junction or surface layers was addressed separately, since we wished to separate and compare conventional, diffused junctions with epitaxially grown junctions. The general structure which we have selected is shown in Fig. 6 with the specific thickness values of the layers given in the inset. The layer X_B is included to provide a "buffer" between the substrate and the layer X_A and an exponential doping gradient to provide a built-in electric field to move photogenerated carriers away from the substrate and toward the junction.

Structures representative of those given in Fig. 6 were grown, and junction layers were formed by a gaseous ($POCl_3$) diffusion. A sufficient number of samples were fabricated to ensure reproducibility of the processes and to obtain average values of the solar-cell parameters associated with each structure. Illuminated solar-cell characteristics representative of the range and average values for each structure are given in Table 1.

Additional results and an interpretation of the data in Table 1 are given in Section IV. The significant result as far as the epitaxial approach is concerned is that only ∿15 μm of epitaxial growth is sufficient to produce

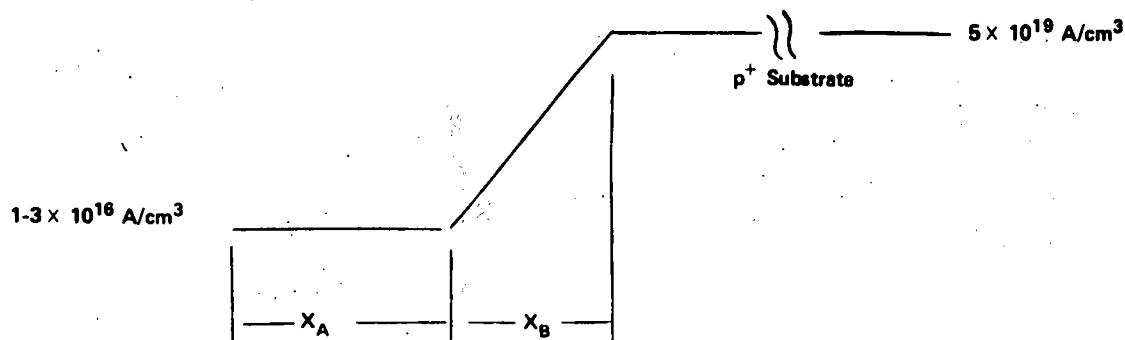

STRUCTURE	X_A	X_B	$(X_A + X_B)$
I	5	12	17
II	10	12	22
III	35	12	47

Figure 6. Concentration profile of epitaxial base layer.

TABLE 1. AM-1 CHARACTERISTICS OF BASELINE DIFFUSED-EPITAXIAL STRUCTURES ON SINGLE-CYRSTAL SUBSTRATES

Range of Measured AM-1 Parameters

Structure	J_{sc} (mA/cm^2) min	J_{sc} (mA/cm^2) max	V_{oc} (mV) min	V_{oc} (mV) max	FF min	FF max	η (%) min	η (%) max	$\overline{J_{sc}}$ (mA/cm^2)	$\overline{V_{oc}}$ (mV)	$\overline{FF}$	$\bar{\eta}$ (%)
I	25.9	28.2	538	605	0.757	0.810	11.2	13.2	27.0	572	0.777	12.2
II	26.2	28.2	548	598	0.772	0.800	11.6	13.7	27.0	572	0.782	12.3
III	26.1	28.6	550	595	0.750	0.806	11.5	13.2	27.6	568	0.785	12.4

solar cells of reasonably high efficiency ($\gtrsim$12%). In our subsequent work, single-crystal substrates of approximately the same resistivity as the low-cost substrate under study were used as controls.

Since one of our overall objectives is to evaluate cells with grown base and junction layers so that the entire cell structure can be grown without the need for a separate junction-formation process, we prepared sets of samples

having epitaxially grown p-type base layers of structures I, II, and III (see Fig. 6) with grown n^+ junction layers. In our initial experiments, the n^+ layers were grown ~1 μm thick and arsenic-doped at ~2 x 10^{18} A/cm^3. Such thick surface layers are not optimum with respect to short-circuit current generation, but are easily reproduced so that relative judgments between structures and substrates can be made. A comparison of the illuminated AM-1 characteristics of solar cells made from such structures grown on single-crystal substrates is given in Table 2.

TABLE 2. AM-1 CHARACTERISTICS OF BASELINE ALL-EPITAXIAL SOLAR-CELL STRUCTURES

Structure	J_{sc} (mA/cm^2)		V_{oc} (mV)		FF		η (%)		$\overline{J_{sc}}$ (mA/cm^2)	$\overline{V_{oc}}$ (mV)	$\overline{FF}$	$\overline{\eta}$ (%)
	min	max	min	max	min	max	min	max			-	
I	21.0	23.4	585	590	0.777	0.777	9.6	10.1	22.4	587	0.735	9.8
II	22.2	24.5	570	579	0.710	0.730	9.4	10.3	23.5	573	0.723	10.0
III	22.7	23.4	555	578	0.710	0.734	9.3	9.8	23.1	567	0.722	9.6

SECTION IV

EPITAXIAL SOLAR CELLS ON LOW-COST SILICON SUBSTRATES

The epitaxial techniques described in Section III were applied to the growth of solar-cell structures on four types of potentially low-cost silicon. A brief summary of the properties of these silicon materials is given in Table 3. In subsections that follow, additional characterizations are given along with a description of the performance of solar cells fabricated using these materials as substrates.

TABLE 3. CHARACTERISTICS OF LOW-COST SILICON SUBSTRATES

Substrate - Vendor	Type	Resistivity (Ω-cm)	Major Impurities Level (ppm)	Major Impurities Nature	Crystallinity	Grain Size (mm)
SILSO - Wacker*	p	4-8	1-5	C	Polycrystalline	1-10
RMS - Union Carbide**	p	~0.06	100-200	C,B,P,Fe	Polycrystalline	3-10
UMG - Dow Corning†	p	~0.02	10-100	Al,B,P	Single crystal	No grains
Cast Silicon - Crystal Systems††	p	~1			Polycrystalline	

*Wacker Chemical Corp., Richardson, TX; SILSO is a brand name.
**Union Carbide Research Laboratory, Tarrytown, NY; RMS is "refined metallurgical grade."
†Dow Corning Corp., Hemlock, MI; UMG is "upgraded metallurgical grade."
††Crystal Systems, Inc., Salem, MA.

A. EPITAXIAL GROWTH AND SOLAR CELLS ON POLYCRYSTALLINE SILICON

1. Material Characterization

Initial experiments on epitaxial growth on polycrystalline silicon were conducted using Wacker polycrystalline (SILSO) wafers. These are nominally 15 to 17 mil thick and 4 to 8 Ω-cm (p-type) resistivity. Since the as-received blanks were saw-cut, comparisons of substrate surface preparation (i.e., etching vs Quso* polishing) were conducted. Typical layers simulating solar-cell

*Registered Trademark of Philadelphia Quartz Co., Valley Forge, Pa.

structures were grown on such prepared surfaces in order to characterize the bulk and surface properties of the epitaxial layers. Figure 7(a) and (b) shows photomicrographs (70X) of the surface structure of 35-μm-thick epitaxial layers grown simultaneously on polished and etched Wacker substrates.

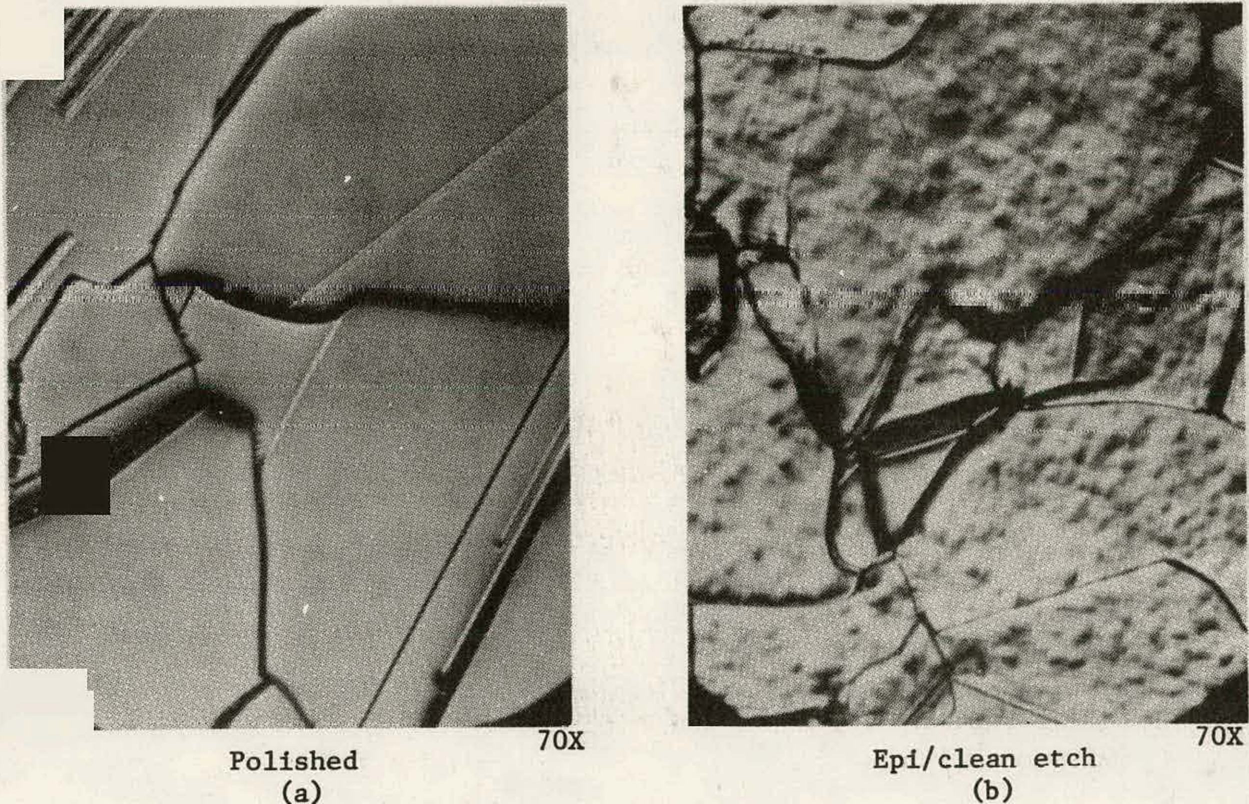

Figure 7. Comparison of the surfaces of 35-μm epitaxial layers grown on (a) polished and (b) etched Wacker polycrystalline substrate.

Section and transmission x-ray topographs were taken to evaluate the relative defect density in the epitaxial films as compared to the substrate. In this case, for ease in the x-ray measurements, a 150-mm-thick film was grown on a chemically etched substrate. Transmission and section topographs of this are shown in Fig. 8(a) and (b) and an enlarged portion of the section topograph is shown in Fig. 9. The topographs clearly show a greatly reduced defect density over most of the epitaxial layer. The few areas where no improvement is observed are generally associated with the nucleation of stacking faults and other line defects with a component inclined to the plane of growth.

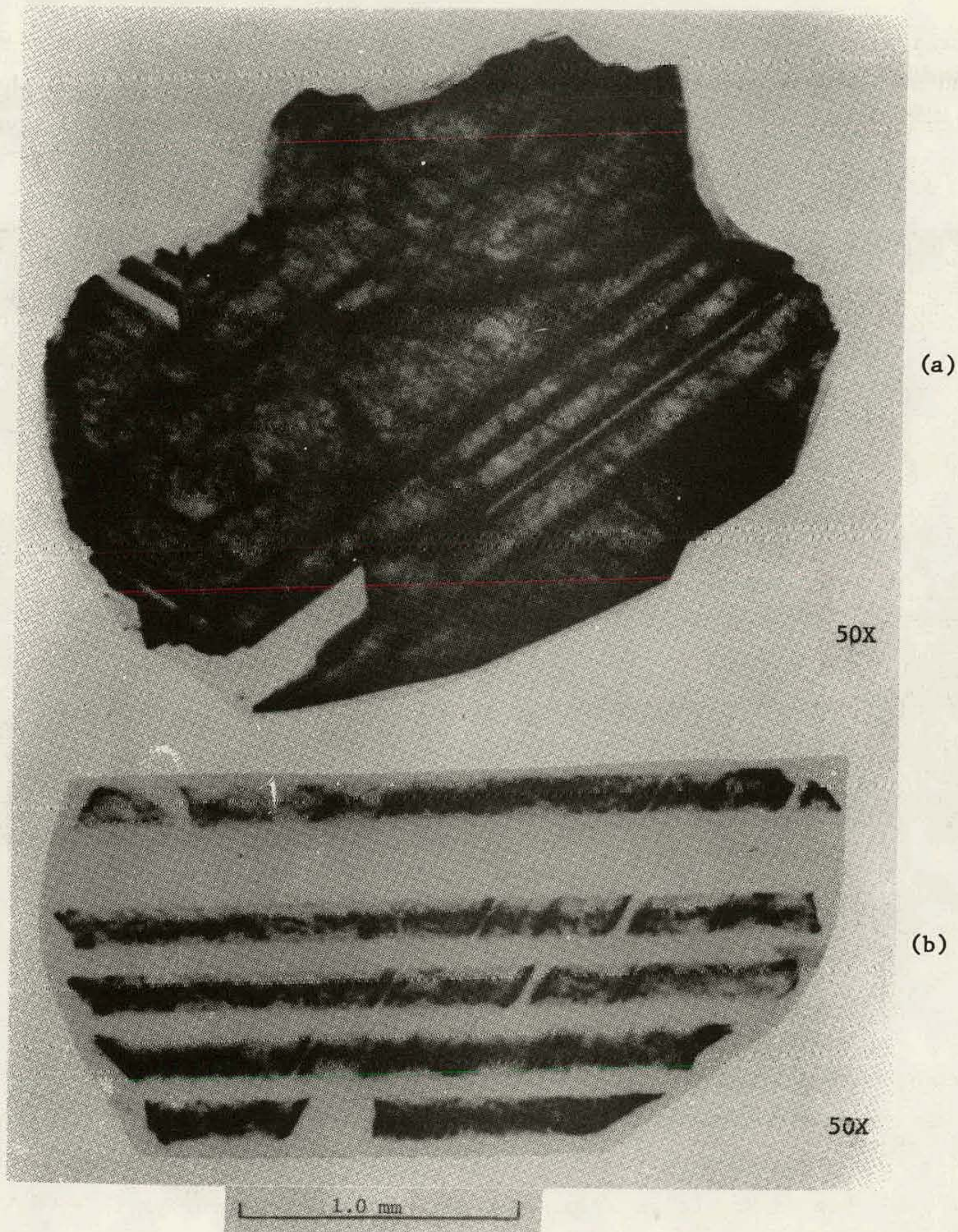

Figure 8. 150-μm-thick film grown on chemically etched substrate. (a) Transmission and (b) section topographs.

Figure 9. Enlarged portion of the section topograph (Fig. 8).

2. Epitaxial Solar Cells - Diffused Junctions

The three structures described in Section III were grown on the Wacker polycrystalline substrates. In each case, both polished and etched surfaces were used, and a control single-crystal sample was included during growth and

processed along with the polycrystalline sample. Problems encountered in the epitaxial growth primarily relate to the surfaces and grain boundaries at the surface. X-ray measurements have shown that the grains in this material are randomly oriented, and we have found, in some cases, preferential growth resulting in uneven surfaces even when the substrates were polished. This effect is dependent to some extent on the surface treatment prior to epitaxial growth. It was found that removal of about 3 to 4 mil of silicon from the surface by chemical etching greatly reduced height differences from grain to grain. A summary of the measured AM-1 solar-cell parameters for samples of each structure is given in Table 4.

TABLE 4. SUMMARY OF SOLAR-CELL DATA FOR EPITAXIAL STRUCTURES GROWN ON WACKER POLYCRYSTALLINE SUBSTRATES

Structure/Substrate Surface	AM-1 Solar-Cell Parameters* J_{sc}** (mA/cm^2)	V_{oc} (mV)	FF ----	η (%)
IP/Wacker Etched	25.1	430	0.58	6.5
IP/Wacker Polished	25.9	555	0.777	7.3
I-Control Single Crystal	25.5	459	0.56	11.5
IIP/Wacker Etched	26.8	535	0.633	9.3
IIP/Wacker Etched	26.9	450	0.531	6.6
II-Control Single Crystal	27.3	563	0.772	12.1
IIIP/Wacker Etched	24.9	485	0.654	8.2
IIIP/Wacker Polished	24.9	500	0.683	8.7
III-Control Single Crystal	28.1	575	0.806	13.0

*AM-1 simulation intensity of 97 mW/cm^2

**All cell areas = 4.4 cm^2

From the results given in Table 4, it can be seen that the limiting factors in the epitaxial cells grown on Wacker substrates are the low values of open-circuit voltage (V_{oc}) and fill factor (FF). Investigations of these devices have given indications that the problem is related to the grain boundaries. Large shunting currents were noted in the junction characteristics and increases

in shunt current occurred when these cells were subjected to normal sintering of the metal contacts. Also, the differing heights of the grains mentioned earlier have caused some problem in metallization resulting in excessive series resistance in some cases.

The short-circuit current densities obtained compared favorably with those measured on the single-crystal epitaxial control cells, and, in spite of the difficulties mentioned above, efficiencies of 5.6 to 9.3% were obtained.

3. Epitaxial Solar Cells - Grown Junctions

Epitaxial structures including the junction layer were grown and processed into solar cells. Surface preparation included either polishing (P) or chemical etching (E). Structures I and II, containing nominally 15- and 20-μm-thick base layers and ∿1-μm-thick n^+ surface layers were grown simultaneously on both the Wacker materials and 10-Ω-cm, p-type, single-crystal control wafers. A summary of the solar-cell performance for these structures is given in Table 5.

TABLE 5. SUMMARY OF CELL PERFORMANCE FOR ALL-EPITAXIALLY GROWN STRUCTURES ON POLYCRYSTALLINE WACKER SUBSTRATES

	AM-1 PARAMETERS						
Sample/Structure	J_{sc} (mA/cm^2)	V_{oc} (mV)	FF --	η (%)	Xj (μm)	$R_\square$ (Ω/□)	Comments
245090-P/I	22.1	525	0.620	7.4	1.1	194	Polycrystalline - surface polished
245366-E/I	22.2	550	0.626	7.8	0.8	242	Polycrystalline - surface etched
244870-Control	24.1	570	0.673	9.5	0.5	177	Single Crystal - 10 Ω-cm substrate
246386-P/II	22.0	520	0.570	6.8	0.8	119	Polycrystalline - surface polished
246874-E/II	22.8	540	0.570	7.3	0.8	150	Polycrystalline - surface etched
246176-Control	24.8	575	0.693	10.1	0.6	172	Single Crystal - 10 Ω-cm substrate

B. EPITAXIAL SOLAR CELLS ON UNION CARBIDE RMS SILICON

1. Material Characterization

The material used in these experiments was obtained from Union Carbide; it is in the form of round wafers (1-1/2 or 2-1/4-in. diam) and is large

grained, randomly oriented, polycrystalline, p-type silicon of ~0.06-Ω-cm resistivity, having chem-mechanically polished surfaces. Projection x-ray topographs of two representative sections of this material with 150 μm of epitaxial silicon growth are shown in Fig. 10. Figure 11 shows a series of section topographs taken at 1-mm spacings in the large grain at the lower right of Fig. 10. An enlargement of several sections of these topographs is shown in Fig. 12. In most areas of Fig. 10 it can be seen that the epitaxial layer (on the left) contains a much lower defect density than the substrate material. However, fractional areas [see Fig. 12(c)] still remain defected. The same observation of improved crystal quality in epitaxial layers was made for the Wacker polycrystalline substrates discussed in subsection A above.

2. Solar-Cell Results - Diffused-Epitaxial Structures

Six RMS wafers were used to grow two each of 15-, 20-, and 50-μm-thick p/p^+ graded cell structures I, II, and III. Control samples were grown for each case on single-crystal p-type substrates of about the same resistivity as the RMS material and (100) orientation.

After the epitaxial growth, solar cells were fabricated by diffusing a phosphorus n^+ junction layer ~0.25 μm deep with a sheet resistance of ~100 Ω/□, metallizing (evaporated Ti/Ag), and mesa etching to define cells of 4.4 cm^2. Spin-on titaniumsilica AR coatings were then applied.

A summary of the measured solar-cell and structural parameters is given in Table 6. An illuminated I-V curve for sample X-13 RMS is shown in Fig. 13. The spectral response was measured for each sample, and the electron diffusion length in the epitaxial base was estimated from the long wavelength portion of the quantum efficiency curve. These data are shown in Figs. 14, 15, and 16.

Additional assessment of this material was made by fabricating solar cells directly by forming a junction by diffusion.

3. *All-Epitaxial Cells on RMS Substrates*

For a complete comparison of structures and materials, all-epitaxial solar cells were fabricated on Union Carbide RMS silicon substrates. Six RMS samples along with single-crystal controls containing a 1-μm-thick epitaxially grown junction layer with base layers of 15, 10, and 50 μm (structures I, II, and III) were fabricated with solar cells and tested. The AM-1 parameters for this series are shown in Table 7. These results for the RMS samples show efficiencies of ~8% with short-circuit current densities not very much lower than

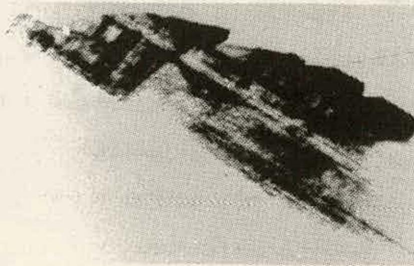

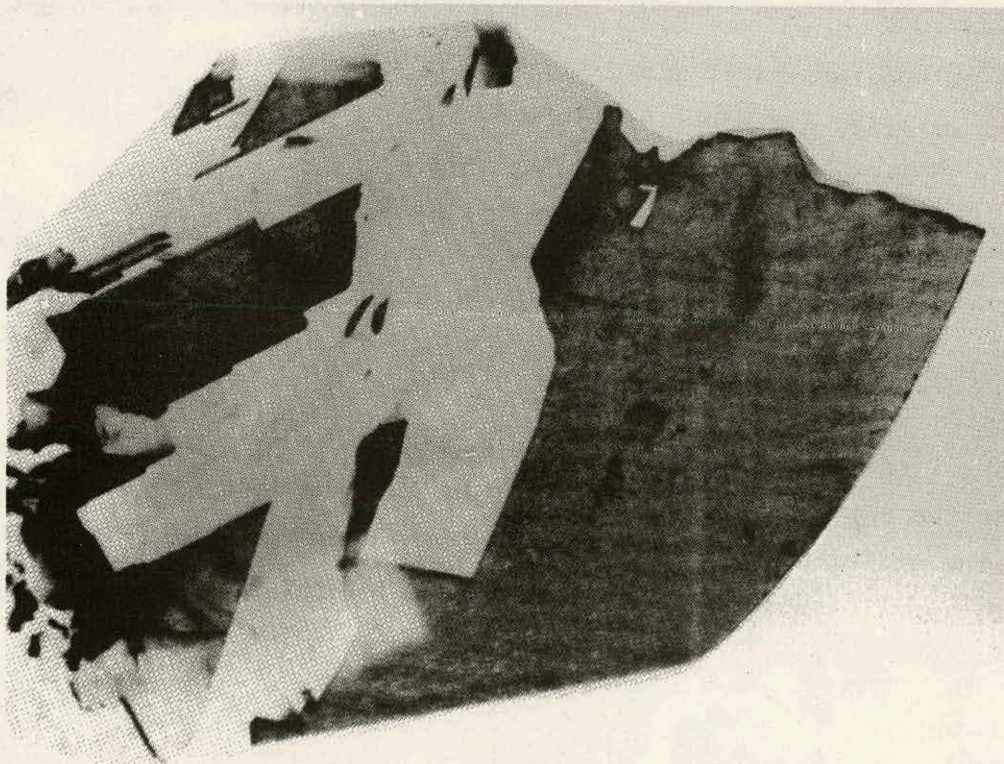

2.5 mm

Figure 10. Projection x-ray topographs of two sections of Union Carbide RMS silicon.

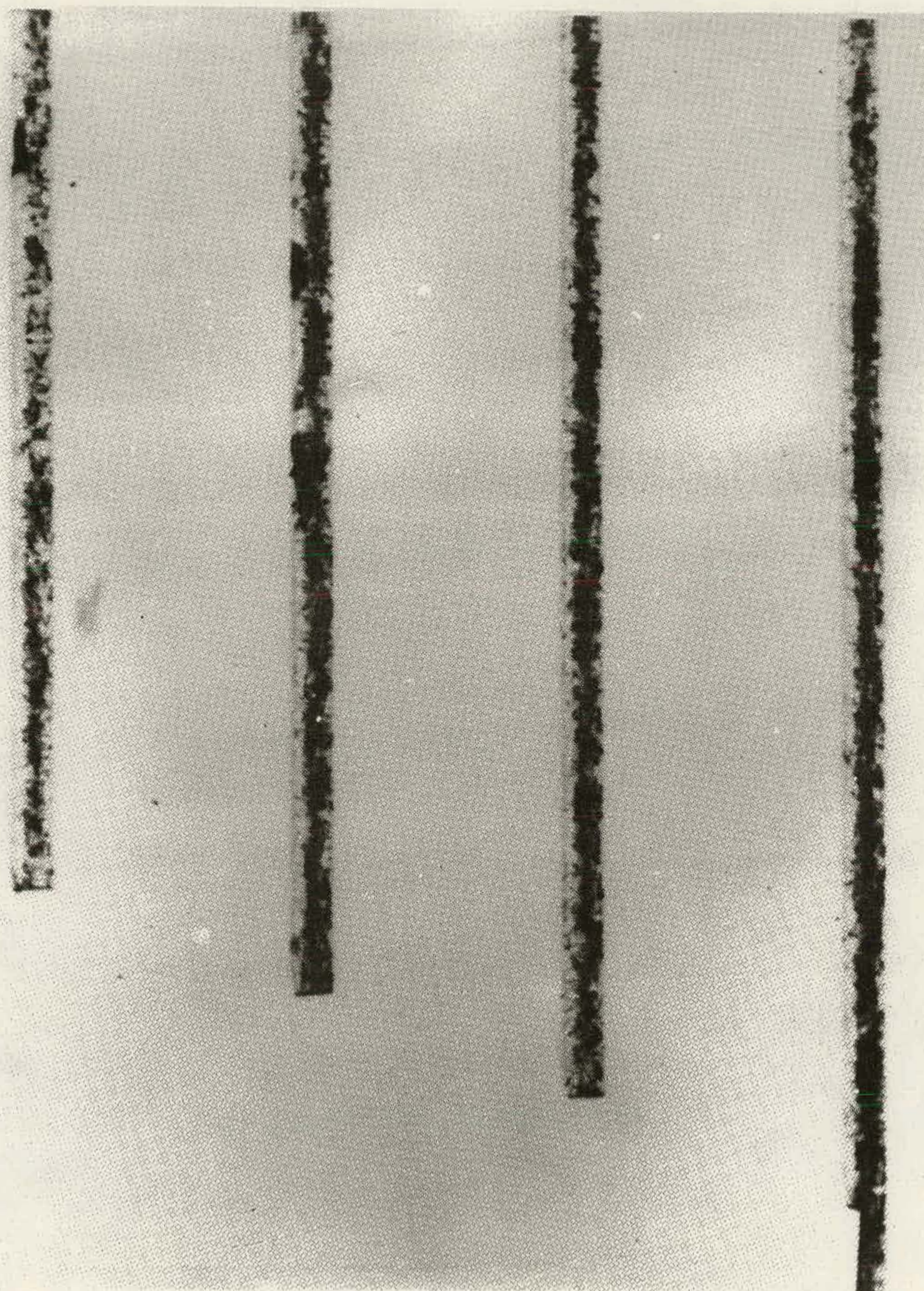

0.1 mm

Figure 11. A series of section topographs of Union Carbide RMS silicon, taken at 1-mm spacings in the large grain at lower right of Fig. 10. Layer is at left edge of each topograph.

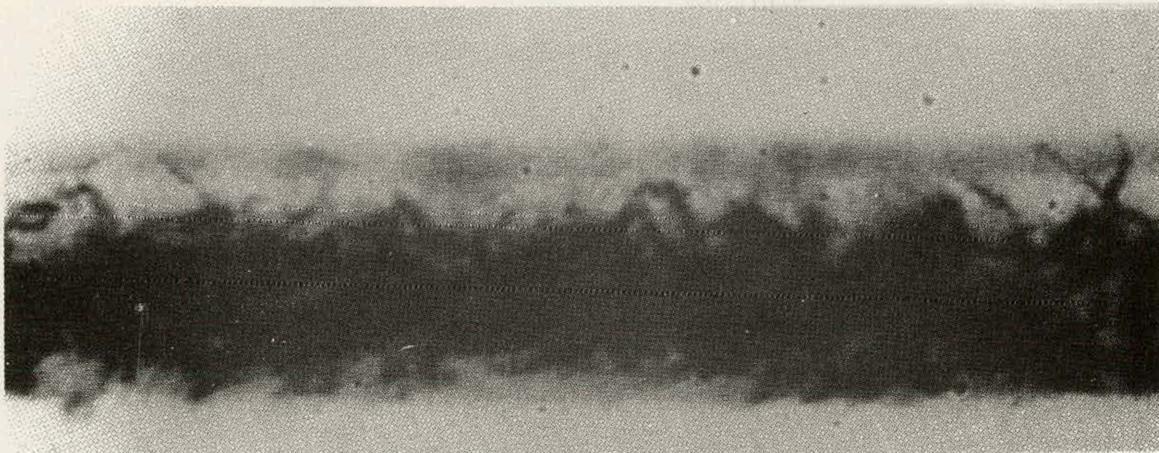
(a)

(b)

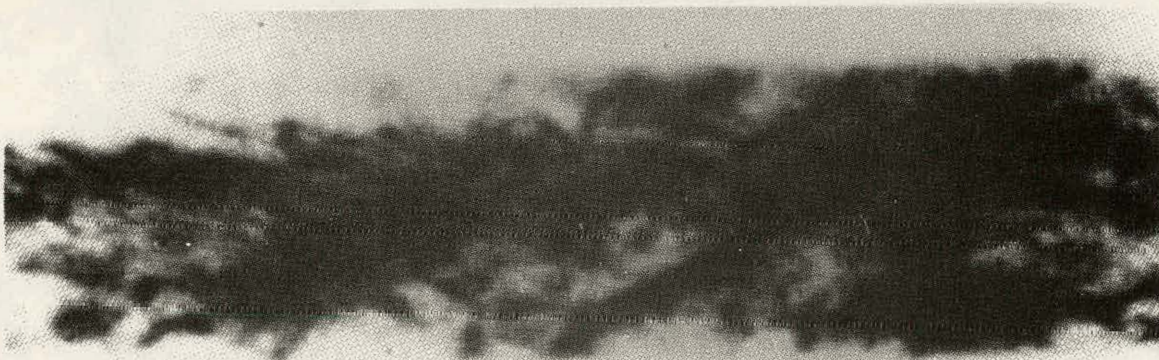
(c)

0.1 mm

Figure 12. Enlargement of several sections of topographs in Fig. 1. Layer is at upper left of each topograph.

TABLE 6. MEASURED SOLAR-CELL AND STRUCTURAL PARAMETERS FOR DIFFUSED-EPITAXIAL STRUCTURES ON UNION CARBIDE RMS SILICON

		AM-1 Parameters*				Diffused Junction	
Sample-Substrate	W_{epi} (μm)	J_{sc} (mA/cm^2)	V_{oc} (mV)	FF --	η (%)	X_i (μm)	$R_\square$ (Ω/□)
X-13 - Single Crystal	14	28.2	578	0.790	13.2	∿0.25	72
X-13 - RMS (1-1/2 in.)	16	25.4	535	0.660	9.3	∿0.25	133
X-13 - RMS (2-1/4 in.)	14	25.0	555	0.745	10.6	∿0.25	71
X-14 - Single Crystal	21	26.7	550	0.770	11.6	∿0.25	132
X-14 - RMS (1-1/2 in.)	20	25.9	538	0.726	10.4	∿0.25	119
X-15 - Single Crystal	47	23.9	535	0.700	9.2	∿0.25	121
X-15 - Single Crystal	47	28.6	562	0.782	13.0	∿0.25	111
X-15 - RMS (1-1/2 in.)	50	25.9	538	0.720	10.3	∿0.25	79
X-15 - RMS (2-1/4 in.)	43	24.3	542	0.717	9.7	∿0.25	117

*ELH lamp simulation at 97 mW/cm^2

the single-crystal controls. However, the fill factors are somewhat more degraded with respect to the controls than for the epitaxial-diffused case (see Table 6). The data for sample 18-2-III suggest that this may be related to grain boundary effects as this sample has smaller grains than all others and has the lowest fill factor and open-circuit voltage. In addition, it has beer

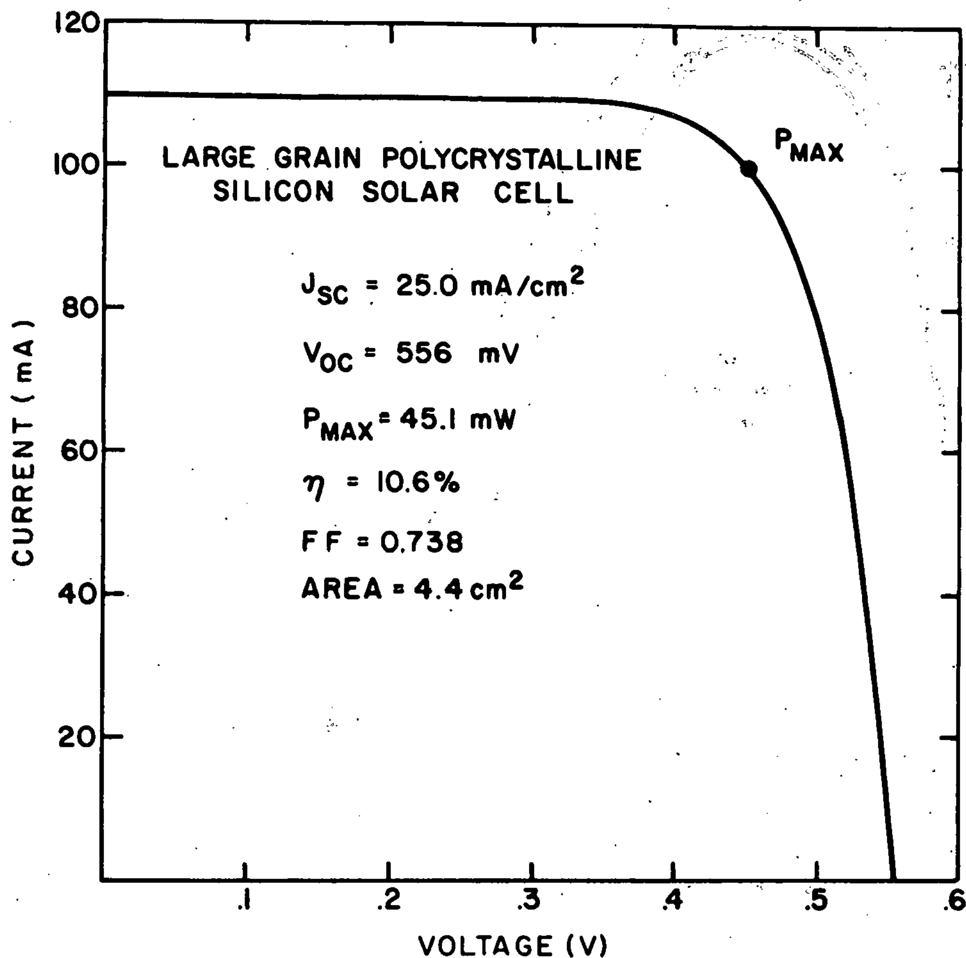

Figure 13. Illuminated I-V curve for sample X-13 RMS

reported in the literature [5,6] that junction formation by low temperature dif-fusion can "passivate" grain boundaries and reduce their effect on cell properties.

---

5. T. H. DiStefano and J. J. Cuomo, Proc. National Workshop on Low-Cost Polycrystalline Silicon Solar Cells, Southern Methodist University, Dallas, Texas, p. 230 (May 1976).
6. J. Lindmayer, Proc. 13th IEEE Photovoltaic Specialists Conference, Washington, D.C., June 1978.

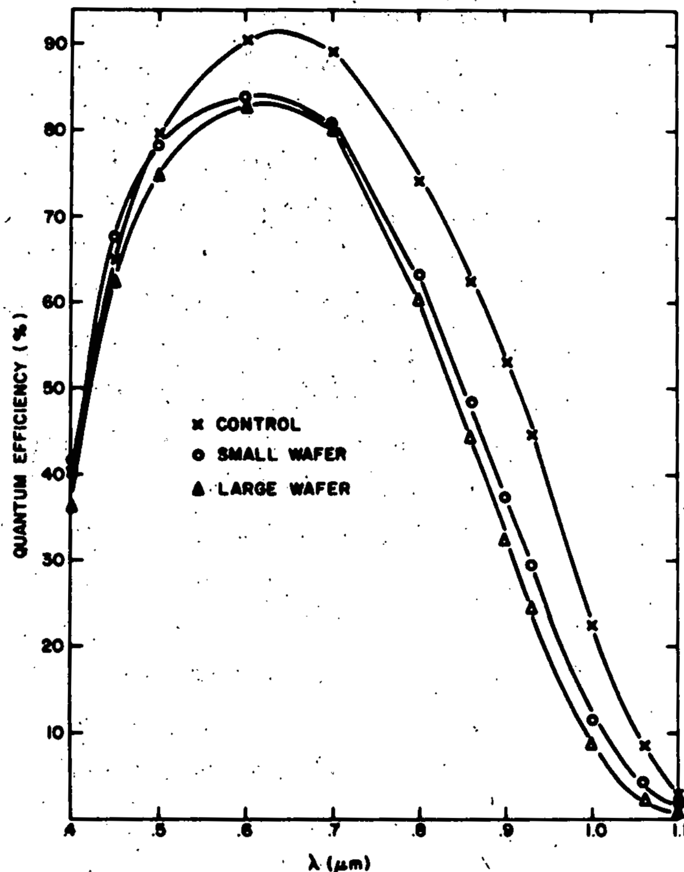

Figure 14. Spectral response curves for diffused-epitaxial structure on Union Carbide RMS silicon, sample X-13.

In comparing the solar-cell performance for the all-epitaxial cells on Union Carbide RMS substrates with the same structures grown on Dow Corning upgraded metallurgical grade silicon (see Tables 7 and 9), it is seen as in the case of the diffused-epitaxial structures that the higher efficiencies result from higher open-circuit voltages and fill factors for the Dow Corning material.

Figure 17 shows the spectral response curves (quantum efficiencies) for all-epitaxial cells on Union Carbide RMS substrates. A curve is shown for three different base widths (structures I, II, and III). The three cells have very similar blue responses as expected, since only the base width is varied. The red response is increased as the base width increases, as it should. In fact, the minority carrier base diffusion lengths calculated from the red portion on the spectral response agree quite well with the widths of the epitaxially grown layers, as seen from the data in the inset of Fig. 17. This

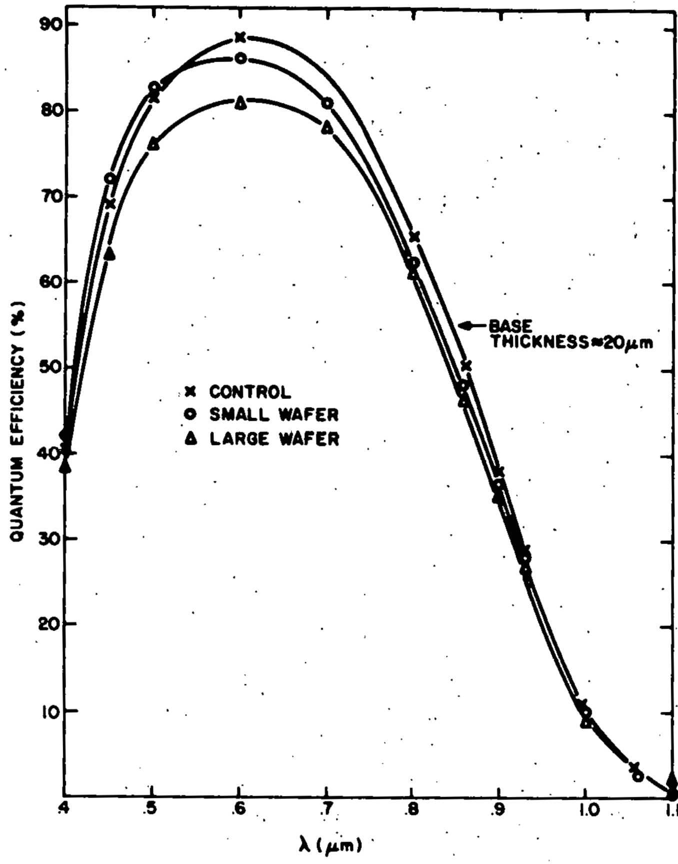

Figure 15. Spectral response curves for diffused epitaxial structure on Union Carbide RMS silicon, sample X-14.

suggests that the apparent "diffusion length" is actually determined by the base width rather than the intrinsic electron diffusion length of the epitaxial material. The overall cell efficiencies or short-circuit currents do not reflect this increased red response, however. For cell 18-3 the benefit of increased red response is cancelled by the poorer spectral response in the middle or peak response portion of the spectrum. The reason for this behavior is not understood.

C. DOW CORNING UPGRADED METALLURGICAL GRADE SILICON

1. Material Characterization

Metallurgical grade silicon substrates, 3.5 cm in diam, were purchased from Dow Corning. This material is p-type with a resistivity of 0.02 Ω-cm with

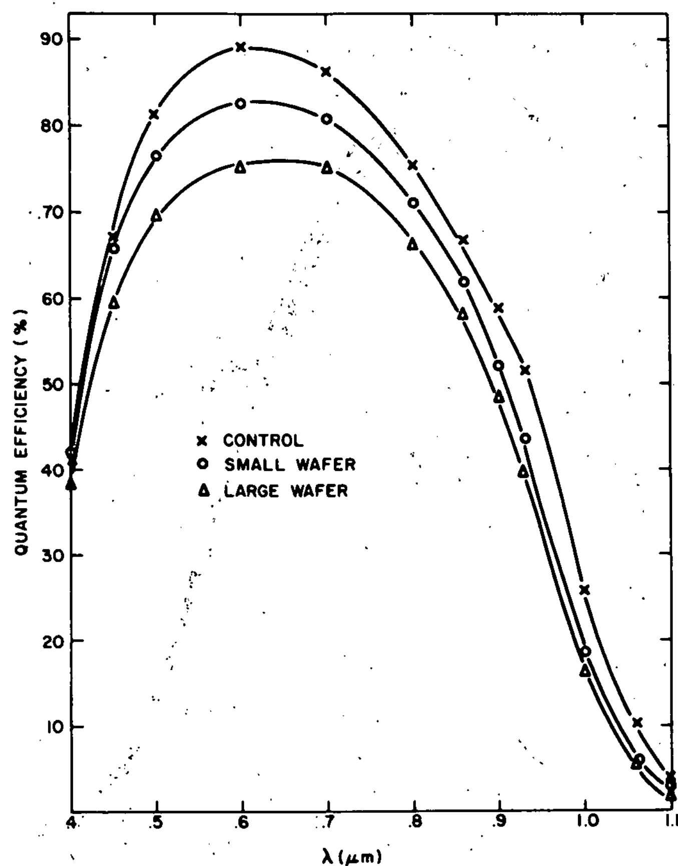

Figure 16. Spectral response curves for diffused epitaxial structure on Union Carbide RMS silicon, sample X-15.

TABLE 7. SUMMARY OF ALL-EPITAXIAL STRUCTURES n/p/p GRADE/p^+ ON UNION CARBIDE RMS SILICON SUBSTRATE

Structure	J_{sc} (mA/cm^2)	V_{oc} (mV)	FF	η (%)
16-1-I Control	23.0	585	0.760	10.6
16-1-I RMS (1½)	21.8	556	0.65	8.1
16-3-I RMS (2¼)	23.1	542	0.68	8.0
17-1-II Control	23.1	562	0.74	9.9
17-2-II RMS (1½)	22.2	540	0.67	8.4
17-3-II RMS (2¼)	20.4	528	0.60	7.3
18-1-III Control	23.3	565	0.73	9.9
18-2-III RMS (1½)*	20.3	500	0.62	6.4
18-3-III RMS (2¼)	20.9	540	0.68	7.8

*This sample has smaller grains than all others.
ELH lamp simulation at 97 mW/cm^2.

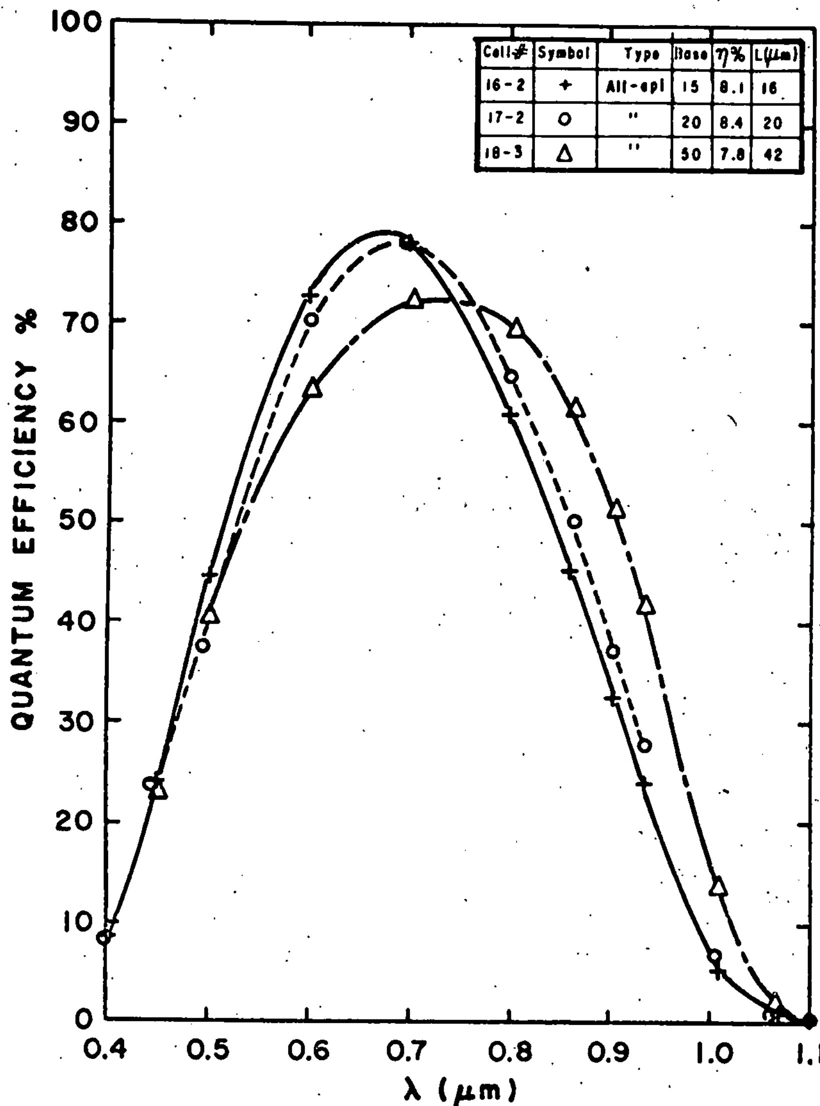

Figure 17. Spectral response for all-epitaxial cells on Union Carbide RMS silicon.

Al, B, and P as the major impurities reported by Dow Corning. Thick epitaxial layers (∿100 μm) were grown and examined using x-ray topographic techniques. The projection topograph (Fig. 18) shows a high density array of misfit dislocations and several stacking faults. This is the first time that we have observed misfit dislocations in silicon; however, such dislocations have been reported in epitaxial growth on silicon substrates heavily doped with boron [7].

7. Y. Sugita, M. Tamura, and K. Sugarawa, J. Appl. Phys. 40, 3089 (1969).

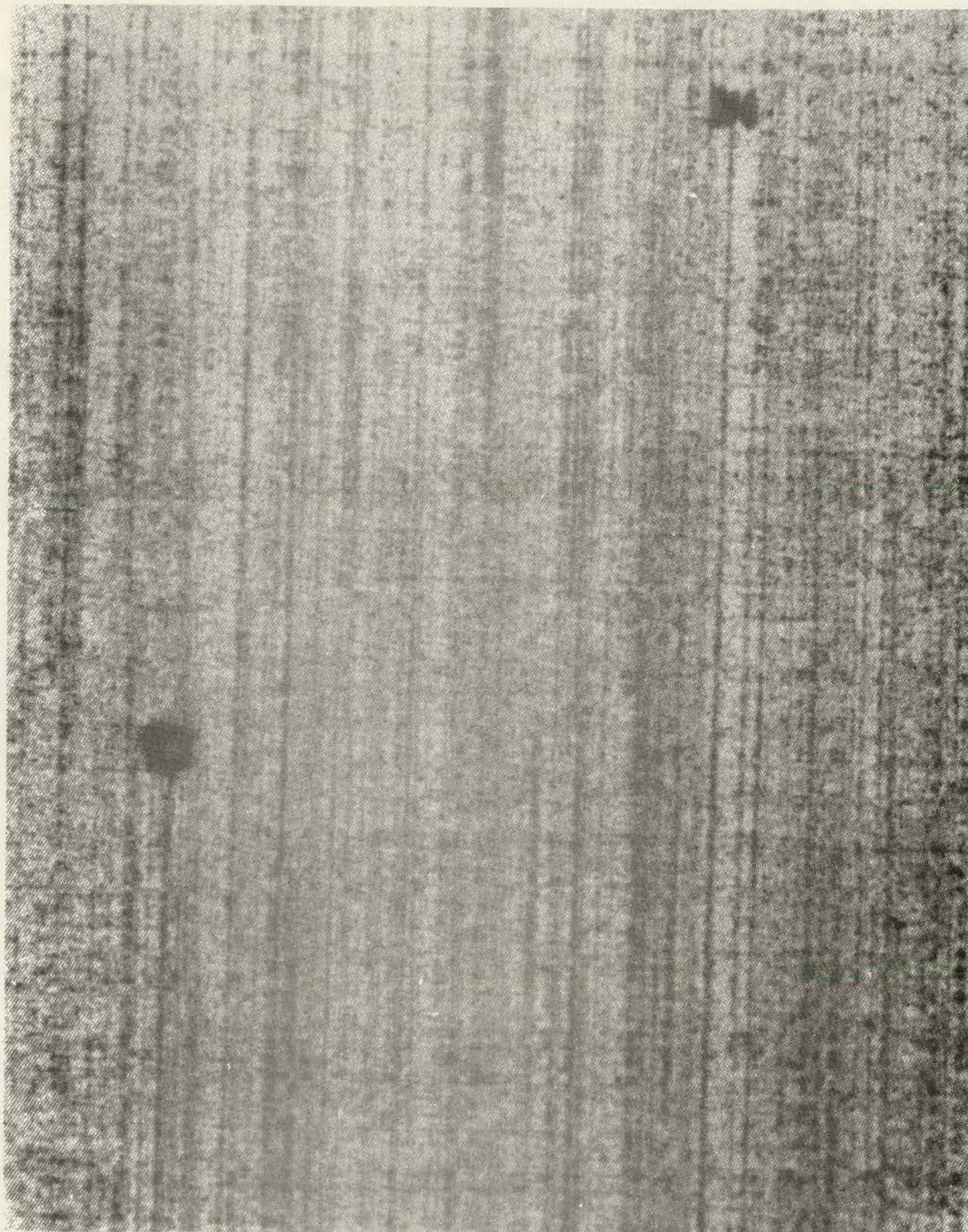

Figure 18. Projection x-ray topograph of a 100-μm-thick epitaxial layer grown on Dow Corning upgraded metallurgical grade silicon.

This effect is also commonly observed in III-V compound growth [8]. Since we do not know the degree of compensation present in this material, the true boron concentration could be considerably higher than indicated by the 0.02-Ω-cm resistivity.

The location of the misfits was determined from section topographs as shown in Fig. 19. As seen in Fig. 19, the misfits are confined to a narrow band at the epitaxial layer and substrate interface. Aside from stacking faults, it can also be seen that the defect density in the epitaxial layer is considerably less than in the substrate.

2. Diffused-Epitaxial Solar Cells

Epitaxial solar-cell structures I, II, and III comprising p/p grade layers were grown on the Dow Corning substrates. In a subsequent step, an ~0.3-μm-deep junction was formed into the epitaxial layers by a $POCl_3$ diffusion. Solar cells of 4.5-cm^2 area were fabricated and tested along with control samples prepared in the same manner but on single-crystal substrates of about the same resistivity as the Dow Corning material.

The AM-1 parameters for these cells are shown in Table 8. These results represent the best efficiencies and cell parameters that we have achieved with a potentially low-cost silicon substrate. For comparison, refer to Table 6 which shows the results obtained with Union Carbide RMS silicon substrates. It can be seen from these data that the higher efficiencies for the epitaxial cells on the Dow Corning material are due primarily to higher open-circuit voltages and fill factors. Since the Dow Corning material is single crystal and the RMS silicon is polycrystalline, it is interesting to explore these differences a little further. For this purpose, the illuminated junction I-V characteristics of epitaxial cells made in Union Carbide and Dow Corning silicon were measured. Typical I-V curves and junction parameters are shown in Fig. 20. For the solar cell on the Dow Corning silicon, the diode n-factor of unity and the low value of saturation current indicate that a good junction was formed and that excess recombination is low. In the case of the RMS silicon, the n-factor is 1.23 and a second slope is seen for voltages lower than 0.465 V, indicating shunt currents or recombination are present. These two effects lower the open-circuit voltage and fill factor and could be related to the polycrystalline nature of the RMS silicon.

8. G. H. Olsen, J. Cryst. Growth 31, 223 (1975).

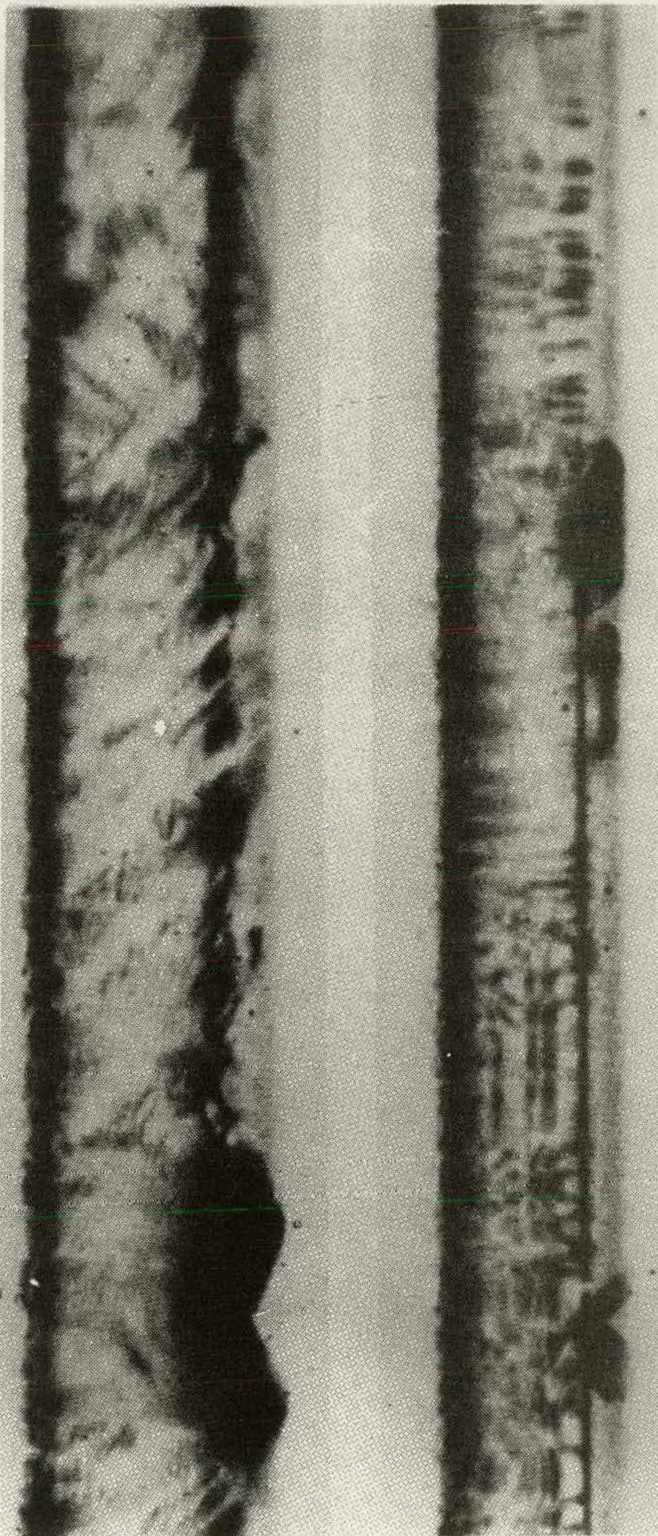

Figure 19. Section x-ray topographs of the crystal in Fig. 18 showing the showing the epitaxial layer (at the right) and the substrate. The dark strain bands in between result from misfit dislocations.

TABLE 8. SUMMARY OF AM-1 CELL PARAMETERS FOR DIFFUSED-EPITAXIAL SOLAR CELLS ON DOW CORNING UPGRADED METALLURGICAL SILICON SUBSTRATES

Substrates/Structure RCA Run #	Base Thickness (μm)	X_j (μm)	J_{sc} (mA/cm^2)	V_{oc} (mV)	FF ----	η (%)
Single-Crystal Control I-25	15	0.3	26.1	605	0.81	12.7
Dow Corning Metallurgical I-25	15	0.3	25.8	602	0.80	12.4
Dow Corning Metallurgical I-25	15	0.3	25.3	610	0.80	12.4
Single-Crystal Control II-26	20	0.3	26.2	598	0.80	12.6
Dow Corning Metallurgical II-26	20	0.3	26.2	605	0.81	12.8
Dow Corning Metallurgical II-26	20	0.3	25.3	610	0.81	12.6
Single-Crystal Control III-27	50	0.3	28.0	595	0.79	13.2
Dow Corning Metallurgical III-27	50	0.3	27.1	592	0.80	12.9
Dow Corning Metallurgical III-27	50	0.3	17.0	598	0.81	12.9

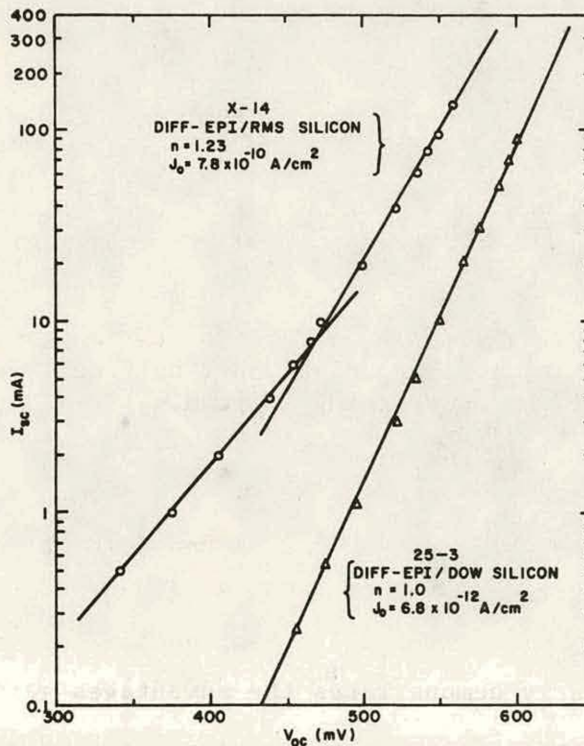

Figure 20. Junction I-V characteristics and parameters for diffused-epitaxial solar cells on Union Carbide RMS silicon (X-14) and on Dow Corning silicon (25-3).

Typical spectral response curves for the cells on the Dow Corning substrates are shown in Fig. 21. As with the case for the Union Carbide material, the apparent base diffusion lengths (listed in the inset) derived from the red response of the curves are approximately equal to the actual base layer thickness.

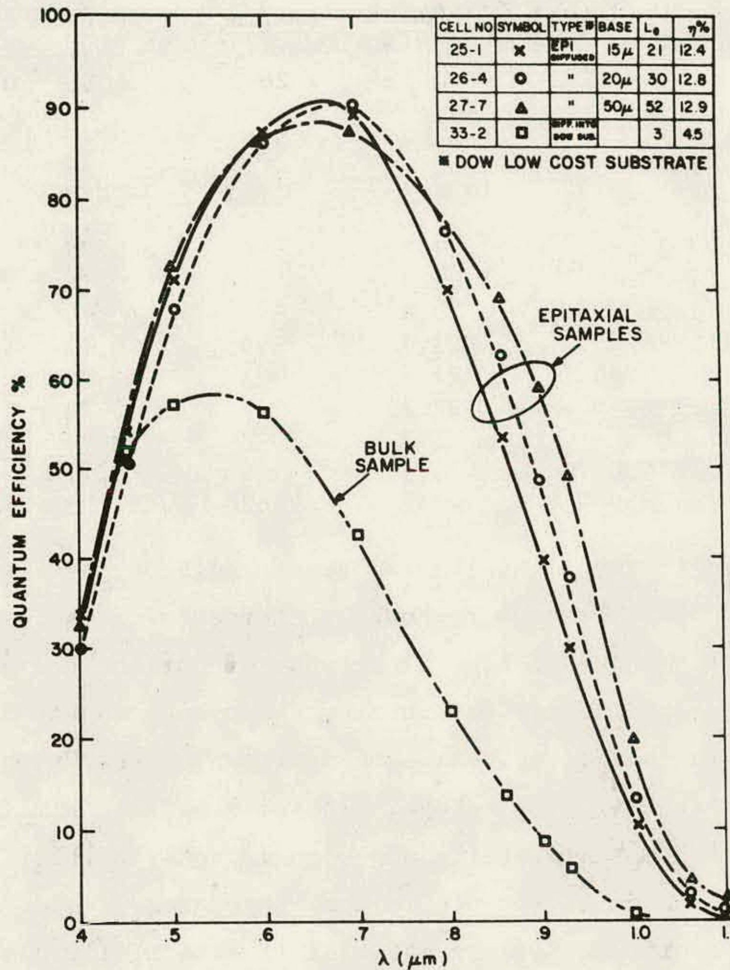

Figure 21. Spectral response curves for three diffused-epitaxial solar cells and a bulk cell fabricated on Dow Corning silicon.

Figure 21 also shows the spectral response for a cell formed by direct diffusion into the Dow Corning material. The blue response for this cell is similar to the epitaxial cells; however, the peak and red responses are significantly reduced. The base diffusion length is only ∿3 μm and the efficiency of this cell cell is 4%. This clearly demonstrates the advantages gained by the epitaxial growth approach for the fabrication of solar cells on such materials.

3. All-Epitaxial Solar Cells

Epitaxial solar-cell structures I, II, and III were grown with 1-μm-thick junction layers. Solar cells were fabricated and tested, and the AM-1 results are shown in Table 9.

TABLE 9. AM-1 SOLAR-CELL PARAMETERS FOR ALL-EPITAXIAL STRUCTURES ON DOW CORNING UPGRADED METALLURGICAL SILICON SUBSTRATES

Substrate/Structure RCA Run No.	J_{sc} (mA/cm^2)	V_{oc} (mV)	FF ----	η (%)
Single-Crystal Control/I-28-2	21.0	590	0.77	9.6
Dow Corning Metallurgical/I-28-1	20.1	571	0.78	9.0
Dow Corning Metallurgical/I-28-3	20.5	576	0.75	8.9
Single-Crystal Control/II-29-5	22.2	579	0.73	9.4
Dow Corning Metallurgical/II-29-4	22.2	583	0.78	10.0
Dow Corning Metallurgical/II-29-6	22.2	577	0.74	9.5
Single-Crystal Control/III-30-8	22.7	578	0.71	9.3
Dow Corning Metallurgical/III-30-7	20.9	558	0.77	9.0
Dow Corning Metallurgical/III-39-9	21.8	562	0.73	8.9

The spectral response of the all-epitaxial solar cells on Dow Corning material is shown in Fig. 22. The blue response of these cells is lower than the epitaxial-diffused cells shown in Fig. 21 because of the thicker junctions.

Another interesting point is that the quantum efficiency curves shown in Fig. 22 are very similar to the all-epitaxial cells grown on the Union Carbide material described in subsection IV.B.3 above. In spite of this similarity, the efficiencies of the all-epitaxial cells are significantly higher for the Dow Corning material. One major difference is that the Union Carbide material is polycrystalline whereas the Dow Corning material is essentially single crystal.

D. CRYSTAL SYSTEMS CAST SILICON SUBSTRATES

1. Material Characterization

Samples from a cast ingot were supplied to us by Crystal Systems, Inc. This material was supplied in saw-cut block-polycrystalline form with large grains of about several millimeters in size; the resistivity is 1 Ω-cm, p-type.

As with previous samples, x-ray topographic analysis were conducted on epitaxial layers grown on this material. The result of this analysis in this case was not as clear-cut as with other silicon forms. Some areas in the epitaxial film did show reduced defect density compared to the cast substrate, (see Fig. 23), but many areas showed no difference between the substrate and

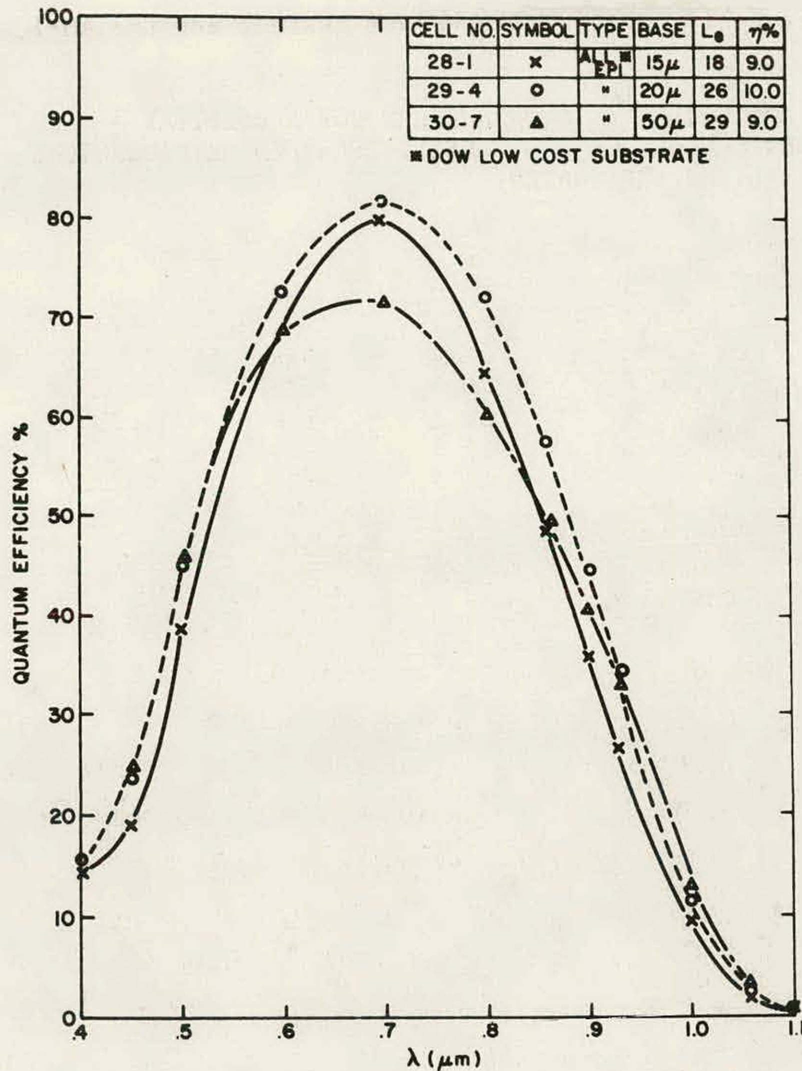

Figure 22. Spectral response curves for all-epitaxial solar cells on Dow Corning silicon.

the epitaxial layer. Although this result is somewhat at variance with what was found in the other forms of low-cost silicon, it is not that surprising since the method used by Crystal Systems to solidify the ingots is considerably different from that used by the other companies. This leads to an uncertainty in the orientation of crystal defects with respect to the cut surface plane and could account for the resultant variable improvements which were observed after epitaxial growth. Also, it should be mentioned that no special efforts were made by Crystal Systems to ensure that this ingot is representative of the material under study by that company.

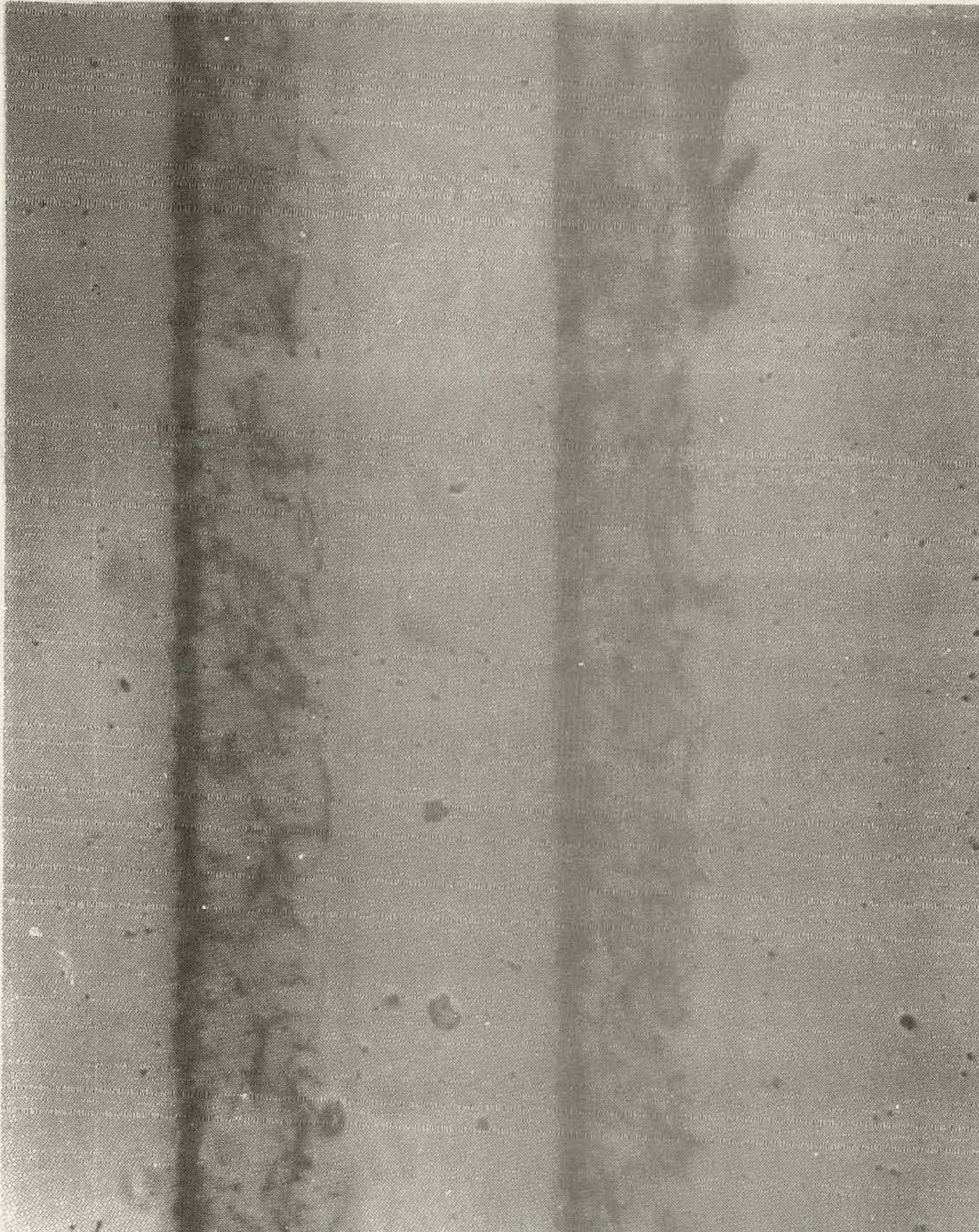

Figure 23. Section topograph, Crystal Systems silicon.

2. Solar-Cell Results

The block from the cast ingot was saw-cut into wafers and the surfaces were etched and polished to form epitaxial substrates. Structures I, II, and III of the all-epitaxial and diffused-epitaxial type were prepared by our standard process. In addition, two cells were fabricated by direct diffusion into this material. The results for solar cells fabricated on these structures along with the controls are given in Table 10. Also listed are the diffusion lengths derived from the measured spectral responses.

Several observations can be made from these data:

- The best efficiency (11.2%) was achieved with an epitaxial structure.
- The diffusion length in the thick epitaxial structures (see samples C.S. III-36-8 and C.S. III-39-8) is considerably longer (28 to 53 μm) than that in the bulk samples (~13 μm) which were prepared by diffusion alone.
- The scatter in the efficiency and cell V_{oc} and FF from sample to sample in the epitaxial structures is large, which is consistent with our observations of variable improvement in defect density in the epitaxial films.

E. DISCUSSION OF RESULTS

Material characterizations, epitaxial growth, and solar-cell device fabrication were performed on five types of silicon substrates. These materials contain crystallographic imperfections, bulk defects, and impurities which are to be expected in low-cost silicon forms. Three of these materials, in fact, represent the present efforts of Dow Corning, Union Carbide, and Crystal Systems to produce a low-cost solar-grade form of silicon. The experimental data presented in this section are then representative of the results obtainable when the epitaxial methods described in this report are used to fabricate solar cells on these substrates.

After examining the data relating to solar-cell performance, we made the following general observations:

- X-ray topographic studies show that the defect density is greatly reduced in an epitaxial layer when compared to the substrate on which it is grown.

TABLE 10. SUMMARY OF AM-1 SOLAR-CELL PARAMETERS FOR CELLS ON CRYSTAL SYSTEMS SILICON

Substrate/Structure RCA Run #	J_{sc}* (mA/cm^2)	V_{oc} (mV)	FF ----	η** (%)	L† (μm)
Diffused-Epitaxial Cells					
C.S. - I-34-1	26.4	530	0.566	9.2	
C.S. - I-34-2	26.1	568	0.726	10.8	20
Single Crystal - I-Control	26.0	570	0.757	11.2	14
C.S. - II-35-4	27.0	566	0.725	11.1	
C.S. - II-35-5	26.2	571	0.746	11.2	20
Single Crystal - II-Control	26.5	580	0.772	12.0	19
C.S. - III-36-7	26.6	535	0.666	9.4	
C.S. - III-36-8	26.4	550	0.715	10.4	53
Single Crystal - III-Control	26.1	570	0.776	11.5	31
All-Epitaxial Cells					
C.S. - I-37-1	22.5	570	0.695	8.9	
C.S. - I-37-2	22.7	585	0.716	9.5	17
Single Crystal - I-Control	23.5	580	0.713	9.7	16
C.S. - II-38-4	22.9	535	0.660	8.1	28
C.S. - II-38-5	23.4	555	0.709	9.1	25
C.S. - III-39-7	22.0	550	0.735	8.9	
C.S. - III-39-8	22.6	552	0.721	9.0	28
Single Crystal - III-Control	22.9	543	0.705	8.8	34
Diffused-Bulk					
C.S. No. 1	22.7	545	0.710	8.9	13
C.S. No. 3	23.1	552	0.712	9.1	13
Single-Crystal Control	30.6	588	0.774	14.0	188

*Total cell area = 4.5 cm^2, illumination = 100 mW/cm^2
**AR coating = spin-on TiO_2/SiO_2
†Obtained from spectral response data

- The superior performance of epitaxial solar cells grown on substrates intentionally doped with Ti compared to cells made directly in the same material implies that either the epitaxial electronic/geometric structure is relatively immune to the presence of Ti or that the level of Ti is considerably lower in the epi-layer than in the substrate.
- The best solar-cell performance (12.9% efficiency) was obtained when upgraded metallurgical grade silicon (Dow Corning) was used as a substrate. This material is single crystal but compensated, and a plane of misfit dislocations was found at the epitaxial layer/substrate interface.
- The efficiency of solar cells made on multicrystalline or polycrystalline substrates was found to be lower (9 to 11%) than that on the single-crystal material. This was generally due to a combination of lower fill factor and open-circuit voltage.
- In every case, solar cells made in epitaxial layers had higher efficiency than cells fabricated directly in the same material.
- In all cases, the growth of only an ∿15-μm-thick epitaxial layer is sufficient to obtain a level of solar-cell performance so that the growth of thicker layers is unwarranted.

F. SUMMARY

The data presented in this section have clearly shown that improved solar-cell performance results from the growth of thin epitaxial layers on RMS silicon. The important features contained in these data are summarized below.

- The growth of only a 15-μm-thick epitaxial layer is sufficient to produce solar cells having efficiencies $\eta > 10\%$.
- Solar cells made into epitaxial layers are more efficient than cells made directly with this material.
- The grain boundaries in this material act to limit cell performance by lowering the fill factor and open-circuit voltage.
- The ratio of efficiencies of epitaxial cells made in this material to efficiencies of the same structures in single-crystal substrates averaged 78.5%.

SECTION V

ADVANCED EPITAXIAL REACTORS

The experimental data presented in the preceding sections have demonstrated that the epitaxial process can produce suitable material properties and high-efficiency solar cells on potentially low-cost silicon substrates. However, our cost analyses show that in order to achieve the objective of an epitaxial manufacturing process for the low-cost, large-scale production of solar cells, new epitaxial reactor designs which are capable of much higher throughput and efficiency are required. Recently, RCA Laboratories developed a proprietary epitaxial reactor [9,10] which allows a significant increase in the power and chemical efficiency of the process, is readily amenable to automation, reduces labor costs, and greatly increases the capacity of the epitaxial processing equipment. The main feature of this new reactor concept known as the RCA Rotary Disc (RD) Reactor in comparison to conventional epitaxial reactors is shown in Fig. 24. The conventional susceptor on the right is a simple extension of a flat wafer holder in which the substrate wafers lie next to each other. It has a heptagonal cross section and is tapered in order to achieve the proper gas flow dynamics when placed in a bell jar. This geometry limits the practical length of the susceptor and thus the number of wafers it can hold to about 35. In the RD reactor, the susceptors are in the form of discs arranged in a stack-like fashion, with the wafers paired and facing each other. This allows for very efficient packing of the wafers, which in present design results in 50 wafers per 25-cm length of reactor. The gas distribution system consists of a specially designed manifold which injects and distributes the silicon-bearing gas in the space between pairs of wafers. Thus, the stack can be quite high and in addition, because of this design, increasing the size of the substrate wafers presents no special problems. An assembled version of a prototype RD reactor is shown in Fig 25.

Because of the above features, the RD reactor has the following advantages over conventional reactors:

(1) There is higher wafer capacity per given volume of reactor space.

(2) Lower power and higher chemical efficiency is provided.

---

9. V. S. Ban, U.S. Patent Nos. 4,062,318 and 4,082,865, assigned to RCA Corporation.
10. V. S. Ban, J. Electrochem. Soc. 125, 317 (1978).

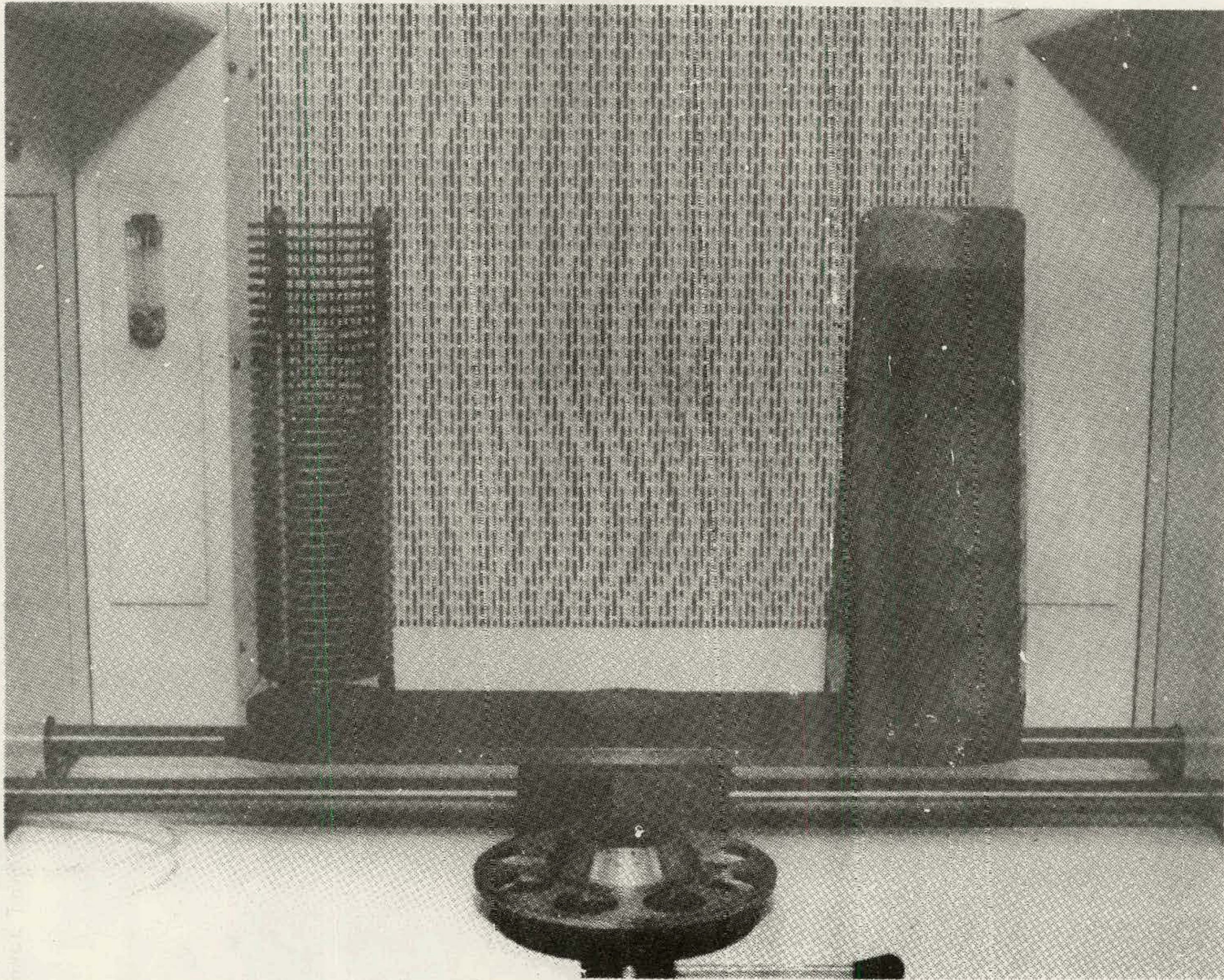

Figure 24. Rotary Disc reactor and conventional epitaxial reactor.

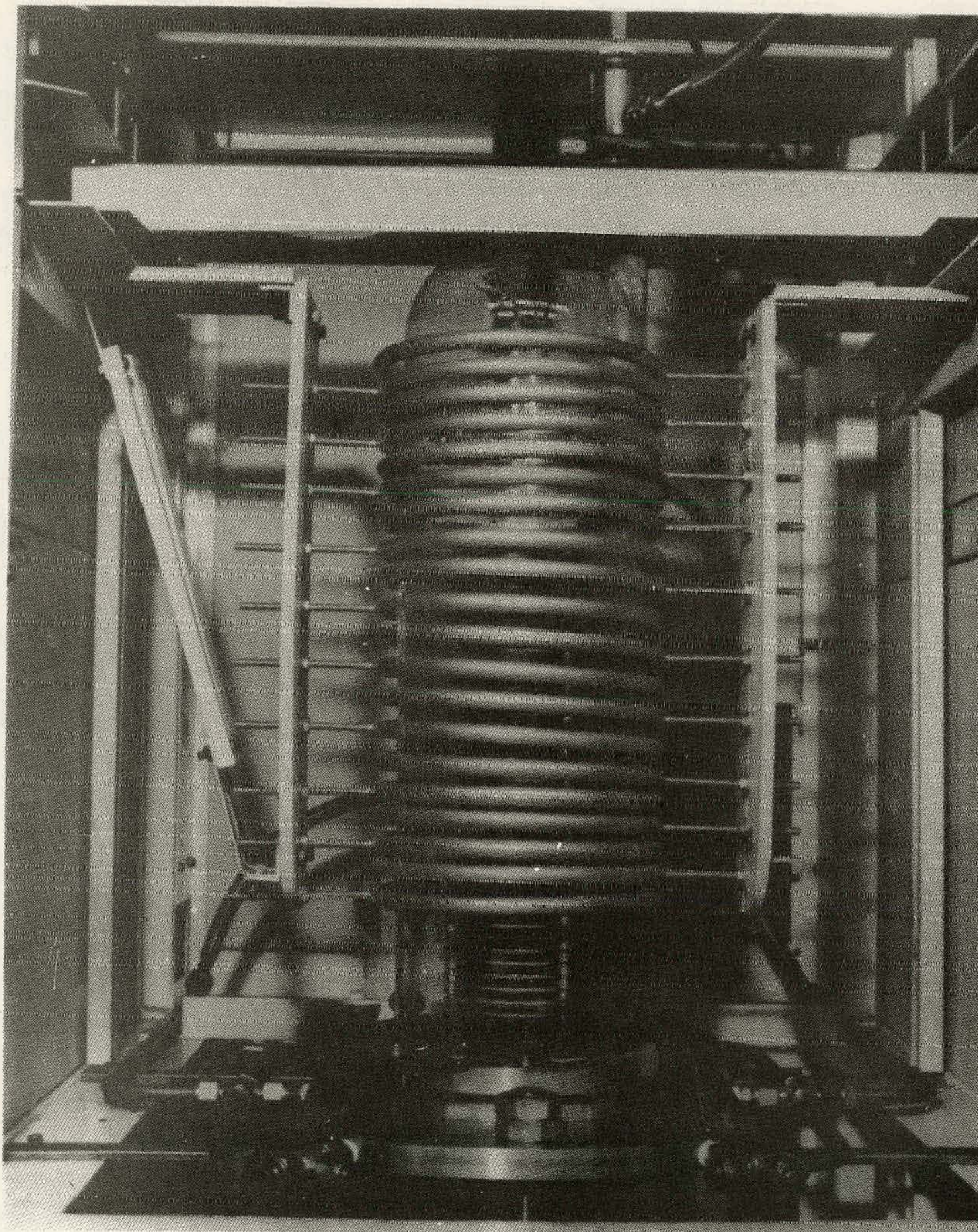

Figure 25. Assembled verson of prototype Rotary Disc reactor.

(3) Better control of thickness and doping uniformity is provided by eliminating the nonequivalency of wafer positions.

(4) There is easy accommodation of large-diameter wafers by a relatively small extension of the susceptor disc diameters.

(5) Due to the relatively small volume of gas between the discs, rapid changes in doping type and/or level are possible; this could lead to structures particularly suitable for solar cells.

(6) The RD reactor is readily amenable to up-scaling and automation to a degree which would lower cost of epitaxy to the level acceptable in solar-cell manufacturing.

During the course of this contract, a prototype laboratory model RD reactor was built and used to qualify this concept for the growth of solar cells. A large scale production model was later assembled and tested.

A series of experimental runs was made in the laboratory model reactor to establish reproducibility from run to run and uniformity of the growth along the stack. This was accomplished and the reactor was then used to grow solar-cell structures. In these experiments, structure I epitaxial base layers nominally 15 μm thick were used throughout, and variations in the thickness and doping profile of the junction layer were made in an attempt to access the conditions required to achieve high-efficiency cells by an "all-epitaxial" process. The following matrix of surface layer structures was grown:

Junction Layer Thickness	Surface Concentration (As)*
0.2 - 1.0 μm	$5x10^{18}$ or $5x10^{19}$

In each run, structures were grown on three Dow Corning upgraded metallurgical grade silicon substrates and one single-crystal p^+ control wafer.

A summary of the samples fabricated along with the measured electrical characteristics of the solar cells is given in Table 11. Although this series of experiments was not exhaustive and solar cells of still higher efficiency should result from further optimization of the growth conditions and structures, the following observation and trends were noted.

- The Rotary Disc (RD) reactor can produce the desired solar-cell structures with good control and uniformity.

*For one junction depth (0.5 μm), graded profile surface layers were also grown.

TABLE 11. SUMMARY OF THE CHARACTERISTICS OF ALL-EPITAXIAL SOLAR CELLS GROWN IN THE ROTARY DISC REACTOR ON DOW SUBSTRATES

		Surface Layer Structure					AM-1 Parameters			
Run No.	Sample Designation	N_s	X_j (μm)	R□ (Ω/□)	Grade	W_B (μm)	J_{sc}	V_{oc}	FF	η
RD071078P1-3	Dow 1	$5x10^{18}$	0.3	210	No		24.7	575	0.751	10.7
RD071078P1-6	Dow 2	$5x10^{18}$	0.3	220	No		25.2	585	0.755	11.2
RD071078P1-7	Dow 3		0.3	200	No		25.1	590	0.763	11.3
RD071078P1-4	Control 4		0.3	260	No	17	24.0	573	0.736	10.2
RD071078A1-3	Dow 5	$5x10^{18}$	0.4	170	No		24.7	570	0.734	10.3
RD071078A1-6	Dow 6	$5x10^{18}$	0.4	180	No		25.3	585	0.763	11.3
RD071078A1-7	Dow 7	$5x10^{18}$	0.4	130	No		24.9	585	0.754	11.0
RD071078A1-4	Control 8	$5x10^{18}$	0.3	290	No	17	24.5	580	0.740	10.5
RD070678P1-3	Dow 9	$5x10^{18}$	0.6	120	No	13	23.1	585	0.773	10.5
RD070678P1-6	Dow 10	$5x10^{18}$	0.6	140	No	14	23.3	590	0.744	10.2
RD070678P1-7	Dow 11	$5x10^{18}$	0.6	120	No	15	24.0	595	0.778	11.1
RD070678P1-4	Control 12	$5x10^{18}$	0.6	180	No	13	22.7	590	0.769	10.3
RD071478A1-3	Dow	$5x10^{19}$	0.2	180	No	17	25.5	581	0.768	11.4
RD071478A1-4	Dow	$5x10^{19}$	0.2	240	No	17	25.2	584	0.751	11.1
RD071478A1-5	Control	$5x10^{19}$	0.2	380	No	17	25.2	581	0.751	10.8
RD071478P1-3	Dow	$5x10^{19}$	0.3	160	No	17	25.8	555	0.593*	8.5
RD071478P1-4	Dow	$5x10^{19}$	0.3	180	No	17	25.5	583	0.763	11.4
RD071478P1-5	Control	$5x10^{19}$	0.3	240	No	17	25.3	580	0.742	10.9
RD071878P1-3	Dow	$5x10^{19}$	1.0	60	No	17	22.5	575	0.751	9.7
RD071878P1-4	Dow	$5x10^{19}$	1.0	90	No	17	22.5	581	0.790	10.3
RD071878P1-5	Control	$5x10^{19}$	1.0	135	No	17	22.7	585	0.782	10.4
RD071278A1-3	Dow	$5x10^{19}$	0.5	290	Yes**	17	25.6	570	0.706	10.3
RD071278A1-6	Dow	$5x10^{19}$	0.5	420	Yes**	17	26.0	547	0.696	10.4
RD071278A1-4	Control	$5x10^{19}$	0.5	400	Yes**	17	24.5	550	0.629	8.5

*Shunted Cell

**$5x10^{19}/1x10^{18}$

- Shallow junction layers $X_j \leq 0.4$ μm are required for efficiencies in excess of 11%.
- There seems to be little difference in cell performance between structures having junction layers with surface concentrations of 5×10^{18} A cm^{-3} or 5×10^{19} A cm^{-3}.
- The graded-profile surface layer ($5 \times 10^{19}/1 \times 10^{18}$ A cm^{-3}) over 0.5 μm results in excessively high sheet resistance which causes low values of fill factor.

SECTION VI

COST ANALYSIS

We have conducted two cost analyses for the production of solar cells by th epitaxial process. The first makes use of technologies now existing or availabl in the near future; the second is a projection of what might be achieved with advanced development of epitaxial reactors based on the concepts described in Section V. The purpose of these analyses is to determine the add-on cost of the epitaxial process and to indicate the integrated cost per watt for a complete process for fabricating solar panels.

To estimate the cost of producing solar panels, a manufacturing sequence generated by RCA [11] under the Automated Array Assembly - Task IV project was used with an appropriately defined epitaxial process introduced to form the active silicon layers.

The analysis was done under the following assumptions:

- Cell efficiency is assumed to be 12.5%. This value was chosen because it has already been achieved on one potentially low-cost substrate.
- Zero cost was assumed for the substrates since little is known about the ultimate cost of the types of silicon used in this work; this assumption is also in line with an analysis to evaluate the add-on cost of processing.
- Production level is 30 MW/yr.
- Assumption specific to the epitaxial process.

The epitaxial reactor is assumed to be similar to that shown in Fig. 25 of Section V, with a throughput for surface preparation, the growth of a 15-μm base layer and the junction layer of two batches of 50 3-in.-diameter wafers per hour. The capital cost for this reactor system is $130 K. The details of these assumptions are given in Table 12.

A summary tabulation showing the results of the cost analysis under the above assumptions is given in Table 13. While the overall cost of $0.46/W is encouraging from the standpoint of the $2/W 1982 goal, the add-on cost of the epitaxy is substantial. It should be noted that this cost is primarily in expense items, the bulk of which comes from the cost of susceptors and the

---

11. R. V. D'Aiello, "Automated Array Assembly," Final Report, DOE/JPL-954352-77/4, December 1977.

TABLE 12. PROCESS PARAMETERS: EPITAXY

PROCESS PARAMETERS: EPITAXY

07/25/78 17:01:23 PAGE 16

ESTIMATE DATE:07/17/78

CLASS:EPITAXIAL GROWTH

CATEGORY:PROCESS DEFINITION   TECHNOLOGY LEVEL:FUTURE   MATERIAL FORM:3" WAFER.

INPUT UNIT:SHEETS   OUTPUT UNIT:SHEETS   TRANSPORT IN:25 SHEET CASSETTE   TRANSPORT OUT:25 SHEET CASSETTE

PROCESS YIELD: 90.0%   YIELD GROWTH PROFILE: 0

INPUT UNIT SALVAGE FACTOR: 0.0   FACTOR GP#: 0   SALVAGE OPTION:FRACTION OF INPUT UNIT VALUE

INPUT UNITS:	0.	0.	0.
FLOOR SPACE,FT**2:	100.	100.	100.

DESCRIPTION: EPITAXIAL REACTOR

ASSUMPTIONS:

1. 3.07" DIAMETER METALLURGICAL GRADE WAFER.
2. RCA EPITAXIAL REACTOR SYSTEM
   SYSTEM COST IS $130.K
   REACTOR $100.K
   LOADER/UNLOADER $30.K
3. 2 BATCHES OF 50 WAFERS EACH PROCESSED PER HOUR.
4. 1 MIL EPI GROWTH. 5 MICRONS/MIN GROWTH RATE.
5. EXPENSE ITEMS:
   HYDROGEN :200 L/MIN X 15 MIN/RUN X 1 RUN/50 WAFERS= 6.0E+4 CM**3/WAFER
   TRICHLOROSILANE: (47.8 CM**2/WAFER * 25.4E-04 CM * 2.33G/CM**3)/
   =0.566 G OF SILICON NEEDED PER WAFER ASSUMING 50% DEP EFF.
   BUT 28G/130G = 22% SILICON IN TRICHLOROSILANE.
   THEREFORE, 0.566G/0.22 = 2.57E+00 GRAMS OF SIHCL3 PER WAFER.
   TRICHLOROSILANE COST IS $.83/LB=1.83E-3$/G.
   HCL: COST IS 1.21E-03 $/G= $.55/LB.
   20 LITERS PER MIN FOR 10 MIN
   2 LITERS PER MIN FOR 10 MIN.
   ----
   220 LITERS PER RUN
   220 LITERS/RUN X 1 RUN/50 WAFERS= 4.40E+3 CM**3/WAFER
   ELECTRICITY: 35 KW X 1/6 HR = 6KWH/RUN X 1 RUN/50 WAFERS
   = 0.12 KWH/WAFER.
   SUSCEPTORS:
   300 RUNS PER DISK X 2 WAFERS/RUN= 600 WAFERS/DISK LIFE
   $30.00/DISK X 1/600= 5.00E-02 $/WAFER.
   MISCELLANEOUS PARTS: ABOUT 1/2 SUSCEPTOR COST/WAFER ESTIMATED.

PROCEDURE

1. WAFERS AUTOMATICALLY LOADED INTO SYSTEM USING LOADER/UNLOADER.
2. EPITAXIAL GROWTH CYCLE LASTS ABOUT 25 MINUTES.
3. WAFERS AUTOMATICALLY UNLOADED USING LOADER/UNLOADER.

INVESTMENTS

INVESTMENT NAME	MAX. THRUPUT UNITS	% INPUT UNITS PROCESSED	FIRST COST	AVAIL.	AREA,FT**2
EPITAXIAL GROWTH SYSTEM	100.00 SH/HR	100.0%	$ 130000.	85.0%	300.
4-POINT PROBE	40.00 SH/HR	10.0%	$ 5000.	90.0%	8.

LABOR

(DL=DIRECT LABOR PERSONS;TL=TOTAL LABOR PERSONS)

NAME	LABOR REQUIREMENTS BASE	# PERSONS/SHIFT/BASE UNIT	THRUPUT/HR/PERSON	% INPUT UNITS PROCESSED
HOURLY OPERATOR	EPITAXIAL GROWTH SYSTEM	2.500E-01		
MAINTENANCE	EPITAXIAL GROWTH SYSTEM	1.500E-01		

TABLE 13. COST ANALYSIS: EPITAXIAL SOLAR PANEL

COST ANALYSIS: EPITAXIAL SOLAR PANEL 12.5% EFF. 07/05/78 11:24:10 PAGE 1

PROCESS COST OVERVIEW-$/WATT

ASSUMPTIONS: 0.717 WATTS PER SOLAR CELL AND 7.8 CM (3") DIAMETER WAFER

CELL THICKNESS: 10.0 MILS. CELL ETCH LOSS: 3.0 MILS. CELL KERF LOSS:10.0 MILS.

STEP	YIELD	PROCESS		MAT'L.	D. L.	EXP.	P. OH.	INT.	DEPR.	SUBTOT	SALVG.	TOTALS	%	INVEST	%
1	100.0%	3.07" METALLURGICAL GRADE WAFER	(A)	0.241	0.0	0.0	0.0	0.0	0.0	0.241	0.0	0.241	21.0	0.0	0.0
2	99.5%	MEGASONIC CLEANING	(B)	0.0	0.005	0.003	0.002	0.000	0.001	0.011	0.0	0.011	1.0	0.004	0.6
3	80.0%	EPITAXY	(B)	0.0	0.059	0.261	0.040	0.040	0.064	0.464	0.0	0.464	40.5	0.449	64.1
4	99.0%	LASER SCRIBING	(B)	0.0	0.002	0.000	0.001	0.001	0.001	0.005	0.0	0.005	0.5	0.010	1.4
5	99.0%	POST DIFFUSION INSPECTION	(A)	0.0	0.015	0.000	0.005	0.003	0.005	0.028	0.0	0.028	2.5	0.033	4.7
6	98.0%	THICK AG METAL-BACK:AUTO	(B)	0.024	0.004	0.005	0.006	0.003	0.004	0.046	0.0	0.046	4.0	0.029	4.2
7	98.0%	THICK AG METAL-FRONT:AUTO	(B)	0.024	0.010	0.012	0.013	0.005	0.008	0.073	0.0	0.073	6.4	0.059	8.4
8	99.0%	AR COATING:SPRAY-ON	(B)	0.002	0.003	0.001	0.003	0.001	0.002	0.011	0.0	0.011	1.0	0.014	1.9
9	80.0%	TEST	(A)	0.0	0.018	0.000	0.006	0.004	0.006	0.034	0.0	0.034	3.0	0.045	6.4
10	98.0%	REFLOW SOLDER INTERCONNECT	(B)	0.002	0.014	0.0	0.004	0.003	0.004	0.028	0.0	0.028	2.4	0.031	4.5
11	99.5%	GLASS/PVB/CELL ARRAY ASSEMBLY	(B)	0.163	0.023	0.0	0.004	0.002	0.004	0.196	0.0	0.196	17.1	0.025	3.6
12	100.0%	ARRAY MODULE PACKAGING	(A)	0.007	0.002	0.0	0.000	0.000	0.000	0.009	0.0	0.009	0.8	0.001	0.1
	57.9%	TOTALS		0.463	0.154	0.282	0.064	0.063	0.100	1.147	0.0	1.147	100.0	0.700	100.0
			%	40.39	13.45	24.62	7.33	5.49	8.72	100.00					

FACTORY FIRST COST,$/WATT: 0.20 DEPRECIATION,$/WATT: 0.01 INTEREST,$/WATT: 0.02

LAND COST,$/WATT: 0.0 INTEREST,$/WATT: 0.0

NOTE: (A)=EXISTING TECHNOLOGY; (B)=NEAR FUTURE; (C)=FUTURE ANNUAL PRODUCTION: 27.2 MEGAWATTS.

345 DAYS OF FACTORY PRODUCTION PER YEAR. 8.00 HOURS PER SHIFT. NO. OF SHIFTS PER DAY VARIES BY PROCESS STEP

HCl gas. The cost of these items and their use factors were based on present practice in the semiconductor industry. For epitaxial reactors dedicated to solar-cell production at the level of 30 MW/yr, volume reduction in the cost of susceptors can be expected, and the use of HCl gas recovery systems should be economically feasible. Moreover, a potentially major economic advantage of the epitaxial process not included in this analysis may have great bearing on the ultimate selection of a low-cost technology. This factor is contained in the development and cost of the silicon substrates. In this work, it was clearly shown that epitaxial layers grown on highly defected substrates have substantially lower defect density as well as better electronic properties than the substrates, and that solar cells of over 10% efficiency have been made in such layers even when the substrates are multigrained. Conventional processing by diffusion or ion implantation on such substrates often results in solar cells with efficiencies of only several percent. Also, the experiments described in the appendix show that the presence in substrates of levels of titanium known to reduce the efficiency of bulk cells by ~35% reduced the efficiency of epitaxial cells by only 12%. These advantages of the epitaxial process will allow the silicon producers a greater latitude in the selection of raw materials and should also result in cost reduction in the purification processes.

To get a feel of what might be possible with future epitaxial systems, a second cost analysis was conducted. For this analysis, a conceptual reactor was designed which makes use of the rotary disc as an element in a continuous, automated process capable of a throughput of ~1000 4-in. wafers/h. With such a system, the add-on cost for the epitaxial process can be reduced to less than $0.10/W.

SECTION VII

CONCLUSIONS AND RECOMMENDATIONS

The work conducted under this contract was directed toward the achievement of three objectives requisite to the ultimate establishment of an epitaxial process for the low-cost, large-scale production of solar cells. These objectives were:

- To determine the feasibility of silicon epitaxial growth on low-cost silicon substrates for the development of silicon sheet capable of producing low-cost, high-efficiency solar cells.
- To achieve a goal of 12% (AM-0) efficient solar cells fabricated on thin epitaxial layers (<25 μm) grown on low-cost substrates.
- To evaluate the add-on cost for the epitaxial process and to develop low-cost epitaxial growth procedures for application in conjunction with low-cost silicon substrates.

These objectives were accomplished. A baseline epitaxial process was developed using single-crystal substrates, and solar-cell structures in the 15- to 45-μm thickness range with efficiencies (AM-1) of 12 to 13.7% were reproducibly demonstrated. This epitaxial process was applied to four potentially low-cost silicon substrates. Improvement in the crystal structure of the epitaxial layers grown on these substrates was demonstrated and solar-cell efficiencies (AM-1) of up to 13% were obtained.

Cost estimates for the large-scale production of solar cells by epitaxial methods using existing or near-future technologies were made, and they indicate that the add-on cost of the epitaxial process is in the range of \$0.55/W. These analyses show that the attainment of high-throughput and high-chemical efficiency is key to the achievement of the long-range cost goals and points out the importance of the development of advanced epitaxial reactor systems. With such systems, the epitaxial costs may be reduced to ∿ \$0.10/W.

The first step toward the development of such reactors was accomplished with the work describing the Rotary Disc (RD) reactor. The operational characteristics and technical feasibility of this reactor for the growth of solar cells were demonstrated and cells of over 11% efficiency were made on one low-cost silicon substrate. This reactor incorporates the features necessary to substantially reduce the add-on cost of the epitaxial process.

The results obtained during this one-year effort have shown that the epitaxial process can produce suitable material properties for high-efficiency solar cells on low-cost silicon forms. In order to make it a technically and economically viable process, two major areas need further research and development. These are:

(1) A full technical qualification and an establishment of supply for the lowest cost silicon substrate consistent with high efficiency, good yield, and reproducibility of solar-cell fabrication.

(2) Development of and the firm establishment of the operation and cost details of an advanced epitaxial reactor (Rotary Disc or equivalent).

Item 1 could follow-up with the silicon manufacturers' whose research samples were explored in the work reported here. However, the lowest cost silicon substrate might involve the direct use of metallurgical grade silicon. Research should be directed toward methods of making metallurgical grade silicon compatible with the epitaxial process, or conversely, epitaxial processes should be explored which can produce useful layers on the lowest cost silicon.

Research and development of epitaxial reactors should be directed toward large-scale, continuous systems capable of high chemical efficiency and throughputs in excess of 1000 wafers per hour. The Rotary Disc reactor could form the elemental basis for such systems.

REFERENCES

1. L. P. Hunt, V. D. Dosaj, and J. R. McCormick, "Advances in the Dow-Corning Process for Silicon," Proc. 13th IEEE Photovoltaic Specialists Conference, June 1978.

2. W. C. Breneman, E. G. Farrier, and H. Morihara, "Preliminary Process Design and Economics of Low-Cost Solar-Grade Silicon Production," Proc. 13th IEEE Photovoltaic Specialists Conference, June 1978.

3. R. V. D'Aiello, P. H. Robinson, and H. Kressel, "Epitaxial Silicon Solar Cells," Appl. Phys. Lett. 28, 231 (1976).

4. H. Kressel, R. V. D'Aiello, E. R. Levin, P. H. Robinson, and S. H. McFarlane, "Epitaxial Silicon Solar Cells on Ribbon Substrates," J. Cryst. Growth 39, 23 (1977).

5. T. H. DiStefano and J. J. Cuomo, Proc. Natonal Workshop on Low-Cost Polycrystalline Silicon Solar Cells, Southern Methodist University, Dallas, Texas, p. 230 (May 1976).

6. J. Lindmayer, Proc. 13th IEEE Photovoltaic Specialists Conference, Washington, D.C., June 1978.

7. Y. Sugita, M. Tamura, and K. Sugarawa, J. Appl. Phys. 40, 3089 (1969).

8. G. H. Olsen, J. Cryst. Growth 31, 223 (1975).

9. V. S. Ban, U.S. Patent Nos. 4,062,318 and 4,082,865, assigned to RCA Corporation.

10. V. S. Ban, J. Electrochem. Soc. 125, 317 (1978).

11. R. V. D'Aiello, "Automated Array Assembly," Final Report, DOE/JPL-954352-77/4, December 1977.

APPENDIX

SOLAR CELLS ON TITANIUM-DOPED SUBSTRATES

Because it is known from previous work [A-1] that the presence of titanium in silicon at a concentration of $\sim 10^{14}$ A/cm^3 causes serious degradation of solar-cell performance and since significant quantities of Ti are found in metallurgical grade silicon, specially prepared substrates purposely doped with titanium were purchased* to assess the effect of Ti on epitaxial solar cells. These substrates are single-crystal, doped at 2 x 10^{14} A/cm^3 with titanium and 10^{17} A/cm^3 with boron.

Epitaxial-diffused and all-epitaxial solar cells have been fabricated and tested for the three structures described in the main body of the report. In addition, three cells were made by direct diffusion into this material. For each of the structures, a single-crystal control having the same resistivity but with no titanium was used for comparative purposes. A summary of these results is presented in Tables A-1 and A-2. The spectral response of cells 19-1 and 19-3 (epitaxial-diffused on single-crystal undoped and titanium doped) are shown in Fig. A-1. Comparing curves, we see that the short wavelength response for the diffused-epitaxial cells is significantly superior to the thick-junction layers in the all-epitaxial cells. The undoped single-crystal cells have better red response than the titanium-doped cells indicating a lower diffusion length in the epitaxial layers grown on the titanium-doped substrates. Analysis of the red response of the data of Fig. A-1 shows that the base diffusion length is 27 μm for the control cells and 9 μm for the titanium-doped cells of both types.

Figure A-2 shows typical spectral response curves for cells made by direct diffusion into the titanium-doped silicon and into a bulk control sample. By comparing Tables A-1 and A-2 and Figs. A-1 and A-2, it can be seen that the epitaxial cells are less affected by the presence of titanium than are the bulk-diffused cells. For example, the average short-circuit current density of the titanium-doped bulk cells is 64.5% of the control sample while the average short-circuit current for the epitaxial cells on the titanium-doped substrates is 87.7% of the controls. It should be noted that the degradation

*Dow Corning, Inc., Hemlock, MI.

A-1. R. H. Hopkins, J. R. Davis, P. D. Blais, P. Rai-Choudry, M. H. Haines, and J. R. McCormick, Silicon Materials Task of the Low-Cost Solar Array Project - Phase II, 7th Q. Rep., 954331-77/3, 49 (April 1977).

TABLE A-1. SUMMARY OF RESULTS USING TITANIUM-DOPED SUBSTRATES - EPITAXIAL CELLS

Structure	AM-1* Parameters J_{sc} (mA/cm^2)	V_{oc} (mV)	FF	η (%)	
Diffused-Epitaxial					
19-1-I Single Crystal	27.6	0.586	0.788	13.1	
19-2-I Ti-Doped	24.5	0.580	0.78	11.5	
19-3-I Ti-Doped	24.3	0.580	0.79	11.4	
20-1-II Single Crystal	28.2	0.594	0.80	13.7	
20-2-II Ti-Doped	24.9	0.576	0.78	11.5	
20-3-II Ti-Doped	25.0	0.582	0.78	11.7	
21-1-III Single Crystal	27.3	0.560	0.81	12.8	
21-2-III Ti-Doped	22.7	0.543	0.78	10.0	
21-3-III Ti-Doped	24.3	0.550	0.79	10.8	
All-Epitaxial					
22-1-I Single Crystal	22.7	0.586	0.70	9.6	
22-2-I Ti-Doped	20.1	0.554	0.65	7.4	
22-3-I Ti-Doped	19.1	0.553	0.70	7.7	
23-1-II Single Crystal	24.5	0.570	0.71	10.3	
23-2-II Ti-Doped	20.2	0.548	0.70	7.9	
23-3-II Ti-Doped	20.0	0.545	0.69	7.7	
24-1-III Single Crystal	23.4	0.525	0.39	5.0	←Problem with metallization
24-2-III Ti-Doped	17.9	0.521	0.79	7.2	
24-3-III Ti-Doped	19.5	0.532	0.67	7.2	

*ELH lamp simulation at 97 mW/cm^2

TABLE A-2. CELLS MADE BY DIFFUSION INTO BULK TITANIUM-DOPED SUBSTRATES

Sample No.	Substrate	J_{sc} (mA/cm^2)	V_{oc} (mV)	FF	η (%)
31-1	Ti-doped	17.8	558	0.79	8.1
31-2	Ti-doped	18.0	545	0.77	7.8
31-3	Ti-doped	17.1	542	0.79	7.5
31-4	Control	27.3	628	0.80	14.2

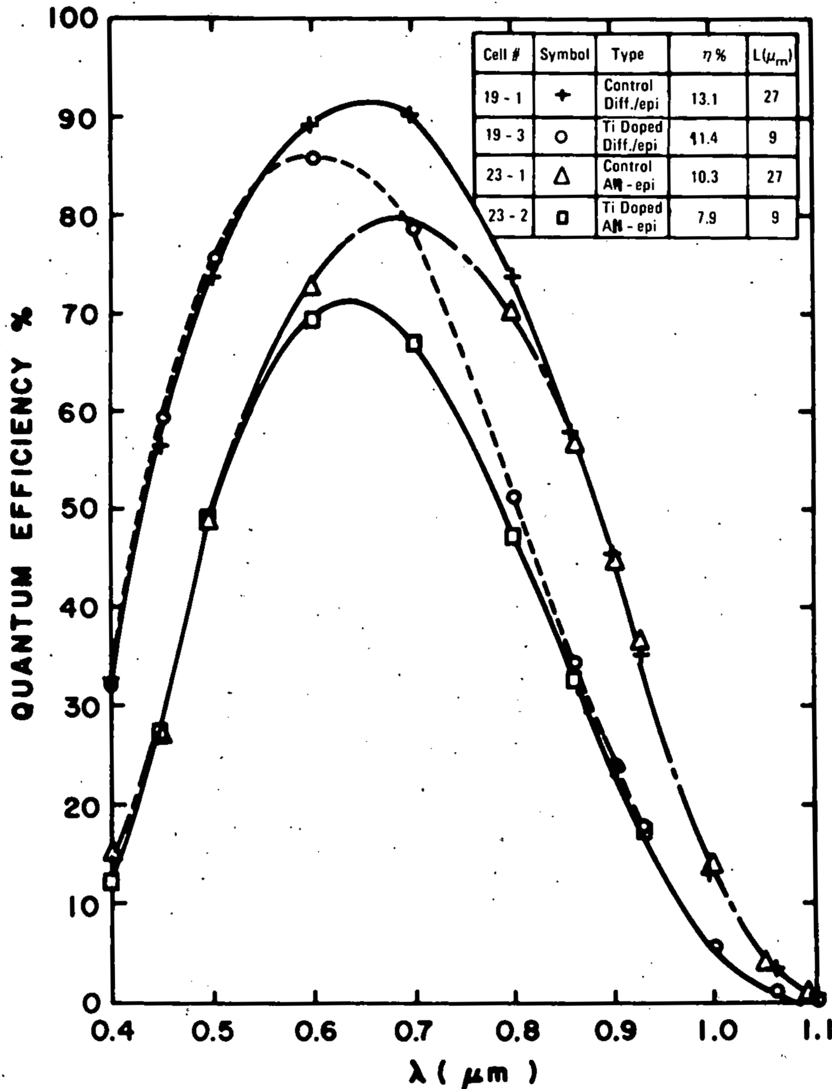

Figure A-1. Spectral response curves for diffused-epitaxial and all-epitaxial cells on undoped and Ti-doped single-crystal substrates.

for the bulk cells is in good agreement (68%) with similar experiments conducted by Westinghouse and Dow Corning [A-1].

The tolerance of the epitaxial cells to the presence of titanium may be related to the base layer thickness. Since the epitaxial cells are thin (15 to 50 μm), they do not depend as much on long diffusion length as do the bulk cells, and, in addition, back surface field effects can enhance the short-circuit current, especially for the thinner epitaxial cells.

It should also be noted that the diffusion length for the epitaxial cells containing titanium is 9 μm as compared to about 5 μm for the bulk cells. This could be due to a lower concentration of titanium in the epitaxial layer compared to the substrate.

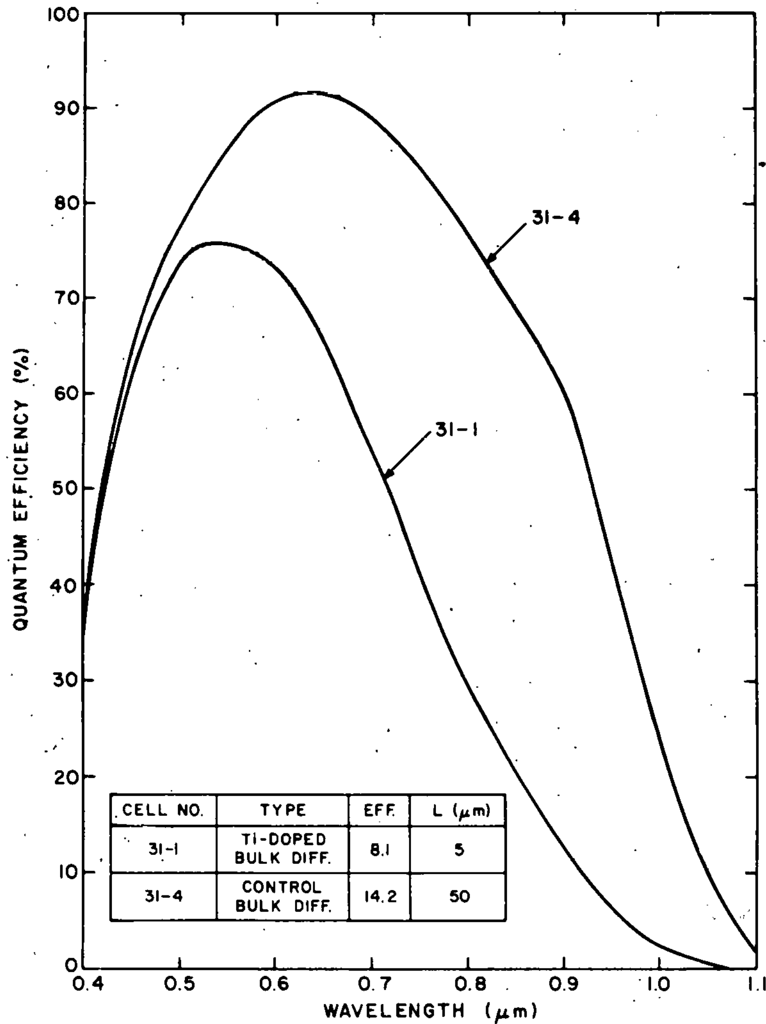

Figure A-2. Spectral response curves for cells made by direct diffusion into Ti-doped silicon and into a bulk control sample.

U.S. GOVERNMENT PRINTING OFFICE: 1980—640-258/1483